

BLOWN UP BY AN EQUILATERAL: PONCELET TRIANGLES ABOUT THE INCIRCLE AND THEIR DEGENERACIES

MARK HELMAN, RONALDO A. GARCIA, AND DAN REZNIK

ABSTRACT. We tour several Euclidean properties of Poncelet triangles inscribed in an ellipse and circumscribing the incircle. We also show that a number of degenerate behaviors are triggered by the presence of an equilateral triangle in the family.

1. INTRODUCTION

Poncelet’s porism is a 1d family of n -gons with vertices on a first conic \mathcal{E} and with sides tangent to a second conic \mathcal{E}_c (also called the ‘caustic’). For such a porism to exist, \mathcal{E} and \mathcal{E}_c must be positioned in \mathbb{R}^2 so as to satisfy ‘Cayley’s condition’ [7]. While the porism is projectively invariant – a conic pair is the projective image of two circles where the ‘Poncelet map’ is linearized, – we have found that Poncelet porisms of triangles ($n = 3$) are a wellspring of interesting phenomena involving the dynamical geometry of classical objects associated with the triangle (centers, circles, lines/axes, etc.).

An emblematic case, shown in [Figure 2](#) (right) is when when $\mathcal{E}, \mathcal{E}_c$ are *confocal ellipses*. In such a porism, – also known as the *elliptic billiard* – the perimeter is conserved [35], and the loci of all four ‘Greek centers’ of the triangle – incenter, barycenter, circumcenter, orthocenter – sweep ellipses [8, 11, 29]. Significantly, neither foci, perimeter, nor triangle centers are projectively equivariant.

Guided by experiment, we have found that certain types of $\mathcal{E}, \mathcal{E}_c$ pairs form equivalent classes of Euclidean phenomena. One criterion is whether the pair is concentric and axis-aligned or not. Relevant for the present study, is a subdivision of triangle porisms based on whether either Poncelet conic is a circle or not. Referring to [Figure 1](#), we obtain the following four combinations:

- (1) Both conics are circles: this is Chapple’s porism [3]. Loci of its *triangle centers*, e.g., incenter X_1 , barycenter X_2 , circumcenter X_3 , orthocenter X_4 (the X_k notation, used here, follows [18]), have been studied in [13, 14, 21, 26]. See [Figure 2](#) (left).
- (2) Only \mathcal{E} is a circle. This system, always an affine image of (4), lends itself to a symmetric parametrization which is at the basis of our analysis. Aspects of its geometry and phenomena are analyzed in [Appendix C](#).
- (3) Only \mathcal{E}_c is a circle: here we will tour its manifold Euclidean properties.
- (4) Neither is circular: Euclidean phenomena are sparser, some are still discernible, e.g., the locus of certain centers are always conics, the locus of barycenter X_2 and orthocenter X_4 always homothetic to \mathcal{E} (see below), etc.

For case (3), we start by identifying triangle centers whose loci are conics. In [17] we show that the locus of a triangle center which is a fixed linear combination of the barycenter and the orthocenter is a sufficient condition for that center to sweep

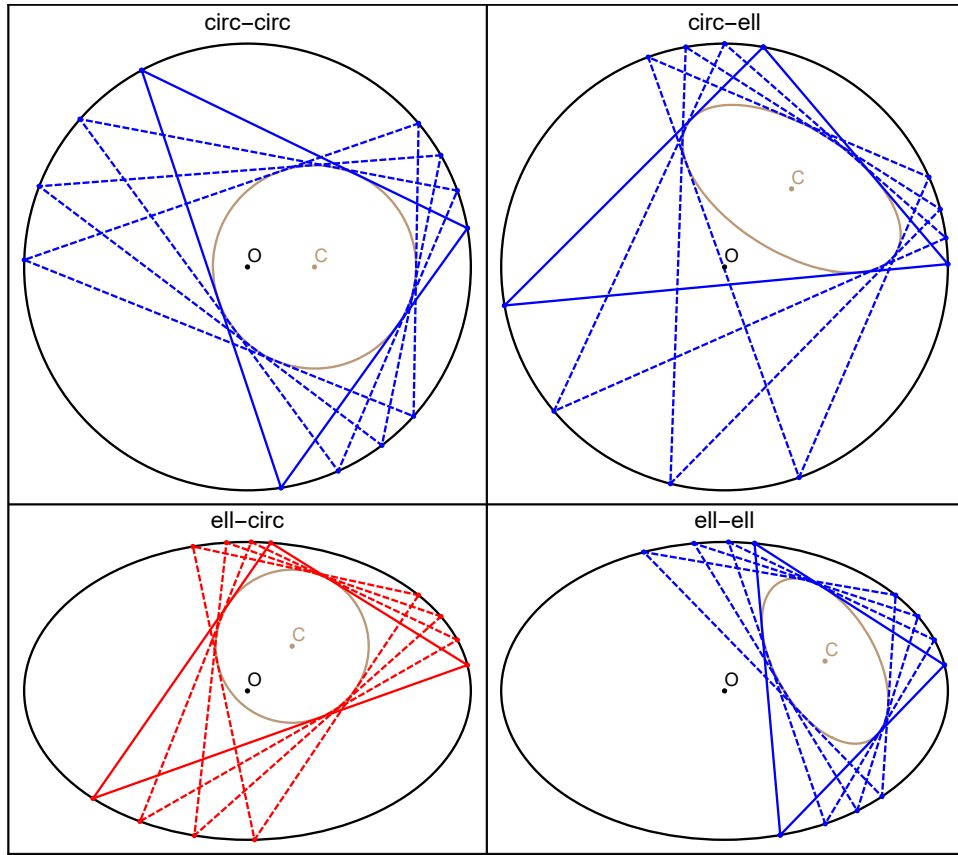


FIGURE 1. **upper left**: outer and inner Poncelet conics $\mathcal{E}, \mathcal{E}_c$ are circles (Chapple's porism); **upper right**: outer \mathcal{E} is a circle; **bottom left**: inner \mathcal{E}_c is a circle (in red since focus of present work); **bottom right**: neither \mathcal{E} nor \mathcal{E}_c is a circle. [Video](#)

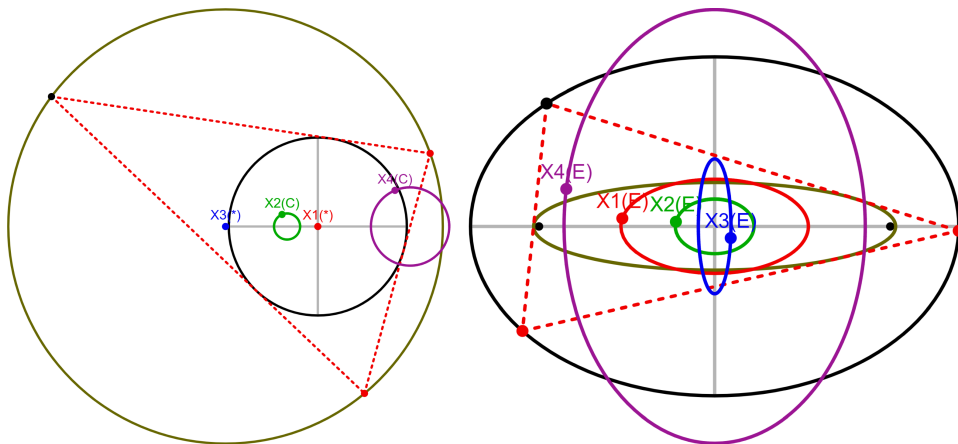


FIGURE 2. **left**: the loci of triangle centers $X_k, k = 1, 2, 3, 4$ over Chapple's porism, studied in [21]. [live](#); **right**: elliptic loci of said triangle centers over the confocal family, studied in [27]. [live](#)

a conic. Nevertheless, other centers may still sweep conics for some choices of conic pairs. Still lacking a predictive theory for the latter, we use numerical methods to pinpoint their conic loci, as in [11].

Below we describe many curious dependencies between the shape and foci of certain loci and the geometry of either Poncelet conic. A surprising find has been that the presence of a single equilateral triangle in the family triggers a host of harmonious degeneracies.

1.1. Article structure. We begin with [Section 2](#), describing two algebraic tool-kits used throughout the paper:

- [Section 2.1](#): we derive the ‘Cayley’ condition for closure of a triangle family inscribed between an ellipse \mathcal{E} and a circle \mathcal{K} (center C), and provide an explicit expression for the caustic radius as a function of the ellipse data. We then visualize the quartic C -isocurves of the radius of K .
- [Section 2.2](#): we present a parametrization for Poncelet triangles inscribed in the unit circle in \mathbb{C} which keeps the intrinsic symmetry of the vertices, using the work on ‘Blaschke products’ from [4]. We then present the generalization to Poncelet families of convex triangles inscribed between any two ellipses as described in [17], and then specialize it to the case where the inner ellipse is a circle, providing explicit formulas.

These are our main results:

- [Section 3](#): we characterize remarkable properties of loci of certain triangle centers, including the barycenter, circumcenter, orthocenter, Euler center, and the Gergonne and Nagel points, denoted X_2 , X_3 , X_4 , X_5 , X_7 , and X_8 , respectively, after [18]. The behaviors include:
 - Axis-alignment, concentricity, and homothety with respect to \mathcal{E} .
 - The ‘railing’ of the foci of certain centers to the axes of \mathcal{E} or to the caustic center C .
 - Circularity: for no obvious reason, some centers always trace circles, regardless of C . X_{36} , the inversive image of the incenter (stationary in our case) with respect to the (moving) circumcircle is always a circle. We derive expressions for its center and radius.
- [Section 4](#): A series of curious, ‘degenerate’ phenomena occurs if the Poncelet family contains an equilateral triangle. This is tantamount to C lying on a special ellipse \mathcal{E}_{eq} which is the locus of the centroids of all equilaterals inscribed in \mathcal{E} , and derived in [34]. The following facts arise:
 - (1) C is a vertex of the locus of X_3 .
 - (2) The locus of X_5 collapses to a segment.
 - (3) The Feuerbach point X_{11} becomes stationary on the incircle, and the reflection of the incenter about it (X_{80}) is a fixed point on \mathcal{E} .
 - (4) The aspect ratio of the loci of the circumcenter X_3 and the Gergonne point X_7 are invariant over all C on \mathcal{E}_{eq} .
 - (5) The locus of X_{36} becomes a straight line (infinite radius circle).
 - (6) The locus of X_{59} , the ‘isogonal conjugate’ of X_{11} (a type of inversive transformation [37]), normally a high-degree curve, collapses to an ellipse touching \mathcal{E} at a special point.
- [Section 5](#): the envelopes of both the circumcircle and of the (incircle,circumcircle) radical axis are studied. The former is shown to be the union of two circles

centered on the foci of the X_3 locus; the latter is shown to be always a conic, which degenerates to a parabola if C is on the boundary \mathcal{E}_{eq} . We conjecture that either envelope has a conic component if and only if the Poncelet family circumscribes a circle.

- **Section 6:** by comparing several Poncelet triangle families, we conjecture that the loci of the Gergonne point X_7 and the Nagel point X_8 are conics if and only if (i) the caustic is a circle or (ii) the pair is confocal.
- **Section 7:** we describe four special triangle porisms when \mathcal{E}_c is a circle, that keep key triangle centers stationary: X_1 (on a focus of \mathcal{E}), X_2 , X_4 , and X_7 . We also identify their conservations, some of which generalize to $n > 3$ Poncelet porisms.

The following appendices are provided:

- **Appendix A:** a table of ‘affine triples’ used in various calculations involving loci, reproduced from [17, Table 1].
- **Appendix B:** the loci of several dozen triangle centers are categorized according to one of six remarkable ‘behaviors’: \mathcal{E} -homothety, axis-alignment, focus on C , major (resp. minor) axis through C , and circularity.
- **Appendix C:** a geometric analysis of circle-inscribed Poncelet triangles, or case (2) above; we show that phenomena here are closely related to those in (3).
- **Appendix D:** computational expressions for the semiaxes of the locus of the Gergonne point X_7 .
- **Appendix E:** a table with most symbols used in the article.

An experimental discovery approach “offers the possibility in some instances of formalizing the inductive leaps that the mathematical mind takes when confronted with what seems to be, logically speaking, incomplete evidence” [6, p.210]. This has certainly been the case for us as most phenomena have been discovered via simulation. In some figure captions we include links to videos as well as interactive animations with a custom-built tool [5].

2. PRELIMINARIES

2.1. Cayley closure condition. The Cayley condition specifies whether two ellipses $\{\mathcal{E}, \mathcal{E}_c\}$ admit a Poncelet family of n -gons [7]. Referring to Figure 1 (bottom right), consider a Poncelet triangle family ($n = 3$) inscribed in an ellipse centered at the origin with semi-axis lengths a and b . Let (x_c, y_c) be the center and a_c and b_c be the semi-axes lengths of a ‘caustic’ ellipse \mathcal{E}_c nested within \mathcal{E} , and let θ_c be the angle of its major axis with respect to the ‘horizontal’ major axis of \mathcal{E} .

In the calculations below, $c_c^2 = a_c^2 - b_c^2$. Correcting our own expression in [16, formula (3)]:

Proposition 1. *The Cayley condition for the pair $(\mathcal{E}, \mathcal{E}_c)$ to admit an $n = 3$ family is given by:*

$$(1) \quad \begin{aligned} & (a^4 b_c^4 + a_c^4 c^4 + b^4 b_c^4 - 2a^2 b^2 b_c^4 - 2c^4 a_c^2 b_c^2) c \theta^4 - 8a^2 b^2 c^2 x_c y_c s \theta c \theta \\ & + [2c_c^2 (a^2 + b^2) (a^2 y_c^2 - b^2 x_c^2) + 2c_c^2 b^2 a^4 + 2(b^2 b_c^4 - a_c^4 c^2 - b^4 c_c^2) a^2 + 2b_c^2 (a_c^2 c^4 - b^4 b_c^2)] c \theta^2 \\ & + a^4 y_c^4 + b^4 x_c^4 + 2b^2 (a^2 a_c^2 - a^2 b^2 - b^2 b_c^2) x_c^2 + 2a^2 b^2 x_c^2 y_c^2 - 2a^2 (a^2 a_c^2 + a^2 b^2 - b^2 b_c^2) y_c^2 \\ & + (aa_c - ab - bb_c)(aa_c + ab - bb_c)(aa_c - ab + bb_c)(aa_c + ab + bb_c) = 0 \end{aligned}$$

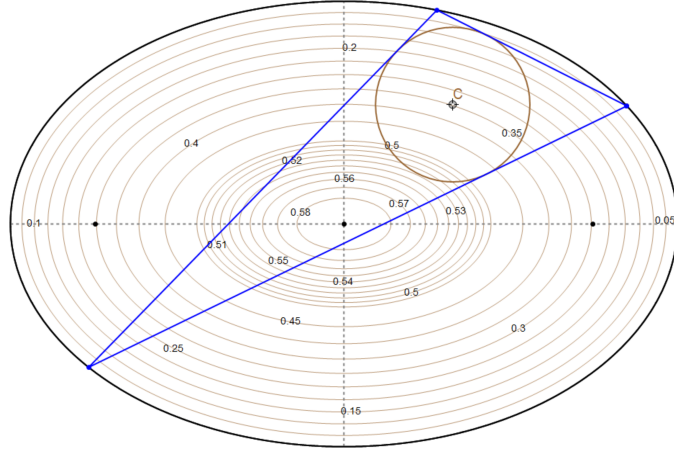


FIGURE 3. The interior of \mathcal{E} is foliated by a family of quartic C -isocurves of caustic radius, $C = X_1$. A particular caustic is shown on the $r = 0.35$ isocurve along with one Poncelet triangle.

where $c\theta = \cos \theta$, $s\theta = \sin \theta$.

Henceforth, let $\delta = \sqrt{(b^4 + c^2 y_c^2)(a^4 - c^2 x_c^2)}$. Referring to Figure 1 (bottom left), we specialize this to a circular caustic:

Proposition 2. *The radius r for an $N = 3$ circular caustic with center at (x_c, y_c) is given by:*

$$r = \frac{b\sqrt{a^4 - c^2 x_c^2} - a\sqrt{b^4 + c^2 y_c^2}}{c^2}$$

Proof. When the caustic is the circle (x_c, y_c, r) , the condition in Equation (1) reduces to a biquadratic on r :

$$c^4 r^4 + 2(b^2 c^2 x_c^2 - a^2 c^2 y_c^2 - a^2 b^2 (a^2 + b^2)) r^2 + (a^2 b^2 - a^2 y_c^2 - b^2 x_c^2)^2 = 0$$

which has four real roots, or four complex roots. The smaller positive root of the above yields a caustic interior to \mathcal{E} . The other positive root $r^* > r$, given by:

$$r^* = \frac{b\sqrt{a^4 - c^2 x_c^2} + a\sqrt{b^4 + c^2 y_c^2}}{c^2}$$

yields a circle which completely encloses or intersects \mathcal{E} , potentially leading to a complex porism. \square

As shown in Figure 3, the expression in Proposition 2 prescribes for the interior of \mathcal{E} a foliation of quartic C -isocurves of caustic radius.

2.2. Symmetric parametrization. Identifying \mathbb{R}^2 with \mathbb{C} , we derived in [16, Def. 3] the following parameterization of Poncelet triangle families inscribed in \mathbb{T} , the unit circle centered at the origin, based on the work in [4] on Blaschke products:

Theorem 1. *For any Poncelet family of triangles inscribed in the unit circle \mathbb{T} and circumscribed about an ellipse with foci $f, g \in \mathbb{D}$ (the unit disk), we can parametrize*

the elementary symmetric polynomials of its vertices $z_1, z_2, z_3 \in \mathbb{T}$ as

$$\begin{aligned} z_1 + z_2 + z_3 &= f + g + \lambda \bar{f} \bar{g} \\ z_1 z_2 + z_2 z_3 + z_3 z_1 &= f g + \lambda (\bar{f} + \bar{g}) \\ z_1 z_2 z_3 &= \lambda \end{aligned}$$

where λ is a parameter that moves along \mathbb{T} .

In order to generalize this parameterization for any Poncelet family of triangles interscribed between two ellipses, we simply apply an affine transformation that takes the unit circle centered at the origin to the desired outer ellipse. Without loss of generality, we can assume that the outer ellipse is also centered at the origin and its major axis is aligned with the real axis of \mathbb{C} .

As before, let \mathcal{E} and \mathcal{E}_c be the outer and inner ellipses of the Poncelet family of triangles and let a and b be the lengths of the semi-major and semi-minor axes of \mathcal{E} , respectively, where \mathcal{E} is axis-aligned and centered at the origin. We can then use the transformation $T : \mathbb{R}^2 \rightarrow \mathbb{R}^2$ defined by $T(x, y) = (ax, by)$ to transform the unit circle into \mathcal{E} . With a slight abuse of notation, this transformation can also be represented in the complex plane, $T : \mathbb{C} \rightarrow \mathbb{C}$, as $T(z) := \frac{(a+b)}{2}z + \frac{(a-b)}{2}\bar{z}$. Moreover, we have $T^{-1} : \mathbb{R}^2 \rightarrow \mathbb{R}^2$ acting as $T^{-1}(x, y) = (x/a, y/b)$ or alternatively, $T^{-1} : \mathbb{C} \rightarrow \mathbb{C}$ acting on \mathbb{C} as $T^{-1}(z) = \frac{(1/a+1/b)}{2}z + \frac{(1/a-1/b)}{2}\bar{z}$.

Label the vertices of our general family of Poncelet triangles as $z_1, z_2, z_3 \in \mathcal{E}$. Defining $\mathcal{E}_{pre} := T^{-1}(\mathcal{E}_c)$ and $z'_i := T^{-1}(z_i) \in \mathbb{T}$ for $i \in \{1, 2, 3\}$, we find that the triangles $\{z'_1, z'_2, z'_3\}$ form a Poncelet family interscribed between the unit circle \mathbb{T} and the ellipse \mathcal{E}_{pre} . We can then apply the previous parameterization of the elementary symmetric polynomials in z'_1, z'_2, z'_3 . This allows us to parameterize any symmetric rational function of the vertices z_1, z_2, z_3 of the general Poncelet triangle family as follows:

Let $P : \mathbb{C}^3 \rightarrow \mathbb{C}$ be a symmetric rational function. Our objective is to parameterize the point $P(z_1, z_2, z_3)$. Since P is symmetric on its 3 inputs, the function $P(T(\cdot), T(\cdot), T(\cdot)) : \mathbb{C}^3 \rightarrow \mathbb{C}$ must also be symmetric on its 3 inputs. Restricting T to the unit circle \mathbb{T} , we can write $T : \mathbb{T} \rightarrow \mathcal{E}$ as $T(z) := \frac{(a+b)}{2}z + \frac{(a-b)}{2}\frac{1}{z}$, which is itself a rational function. Thus, $P(z_1, z_2, z_3) = P(T(z'_1), T(z'_2), T(z'_3))$ is a symmetric rational function on z'_1, z'_2, z'_3 . Write $P(z_1, z_2, z_3) = \frac{P_1(z'_1, z'_2, z'_3)}{P_2(z'_1, z'_2, z'_3)}$ where P_1 and P_2 are symmetric polynomials. By the Fundamental Theorem of Symmetric Polynomials, we can express $P_1(z'_1, z'_2, z'_3)$ and $P_2(z'_1, z'_2, z'_3)$ as polynomials in $\sigma_1, \sigma_2, \sigma_3$ where $\sigma_1 := z'_1 + z'_2 + z'_3$, $\sigma_2 := z'_1 z'_2 + z'_2 z'_3 + z'_3 z'_1$, and $\sigma_3 := z'_1 z'_2 z'_3$. Substituting the symmetric parameterization from [Theorem 1](#), we arrive at a parameterization for $P(z_1, z_2, z_3)$ with $\lambda \in \mathbb{T}$ as the parameter, as desired.

With this method, we have proved many results in [\[16\]](#) and [\[17\]](#) such as:

Theorem 2. *In any Poncelet family of triangles, the loci of the barycenter, circumcenter, orthocenter, nine-point center, and the de Longchamps point are always ellipses. More generally, any fixed linear combination of the barycenter X_2 and the circumcenter X_3 traces out an ellipse as its locus.*

This method is great for proving results such as this, but not so great for finding explicit formulas for the loci. This is due to the fact that everything depends on the foci f, g of the ellipse \mathcal{E}_{pre} which is generally neither of the ellipses $\mathcal{E}, \mathcal{E}_c$ that define our Poncelet family. However, particularizing the case where the inner ellipse

is a circle will allow us to compute such formulas explicitly from the original data of \mathcal{E} and the circle \mathcal{E}_c .

From now on, assume that \mathcal{E}_c is a circle with center $C = x_c + iy_c$ where $x_c, y_c \in \mathbb{R}$ and radius r given as in [Proposition 2](#).

Since T^{-1} stretches the real and complex axis by factors of $1/a$ and $1/b$, respectively, $\mathcal{E}_{pre} := T^{-1}(\mathcal{E}_c)$ is an axis-aligned ellipse with semi-major axis and semi-minor axis equal to r/b and r/a , respectively. In fact, it is a 90° -rotated copy of the outer ellipse \mathcal{E} shrunk by a factor of $r/(ab)$. Therefore its semi-focal length is given by $r \frac{c}{ab}$. Moreover, since ellipse centers are preserved by linear transformations, the center of \mathcal{E}_{pre} is $T^{-1}(C) = x_c/a + iy_c/b$. Since the major axis of \mathcal{E}_{pre} is parallel to the imaginary axis of \mathbb{C} , its foci f and g will be given by $x_c/a + iy_c/b \pm r \frac{c}{ab}$. In order to use the parameterization from [Theorem 1](#) we explicitly calculate their sum and product as

$$\begin{aligned} f + g &= \frac{2x_c}{a} + \frac{2iy_c}{b} \\ fg &= \frac{a^2 + b^2}{c^2} + \frac{2i}{ab} \left(x_c y_c + \frac{1}{c} \sqrt{(a^4 - c^2 x_c^2)(b^4 - c^2 y_c^2)} \right) \end{aligned}$$

We can now calculate explicit formulas for any Poncelet family of triangles where the inner ellipse is a circle. In particular, we can calculate the loci of the barycenter X_2 and the circumcenter X_3 , and then use the table in [Appendix A](#) to explicitly calculate the loci of many triangle centers that can be conveniently written as a linear combination of X_1 , X_2 , and X_3 .

3. REMARKABLE LOCI

In this section, let \mathcal{T} (resp. \mathcal{T}_g) denote a family of Poncelet triangles circumscribing a circle (resp. interscribed between two generic conics $\mathcal{E}, \mathcal{E}_c$). In both cases, let the center of the outer conic be the origin and $C = [x_c, y_c]$ denote the caustic's center.

In [[17](#), Thm.1] we showed that if a triangle center X is a fixed linear combination of the barycenter X_2 and the circumcenter X_3 , its locus over any Poncelet family is a conic. Since over \mathcal{T} the incenter X_1 is fixed:

Corollary 1. *Any center which is a fixed linear combination of the incenter X_1 and a another center which sweeps a conic locus will also sweep a conic as its locus.*

3.1. Loci of $X(\mathbf{k})$, $\mathbf{k}=2,4,7$. The barycenter X_2 (resp. orthocenter X_4) is the meet-point of lines from each vertex to the opposite side's midpoint (resp. altitude foot). The Gergonne point X_7 is the meet-point of lines from each vertex to the where the opposite side touches the inscribed circle. For more information, see [[37](#)].

For next three propositions, refer to [Figure 4](#).

Proposition 3. *Over \mathcal{T} , the locus of X_2 is homothetic to \mathcal{E} . Its center C_2 is collinear with the center of \mathcal{E} and the caustic center C . The center C_2 and semi-axis lengths a_2, b_2 are given by:*

$$\begin{aligned} C_2 &= \frac{2}{3} [x_c, y_c] \\ a_2^2 &= \frac{-4ab(a^2 + b^2)\delta - 4b^4c^2x_c^2 + 4a^4c^2y_c^2 + a^2b^2(a^4 + 6a^2b^2 + b^4)}{9b^2c^4} \\ b_2^2 &= \frac{b^2}{a^2} a_2^2 \end{aligned}$$

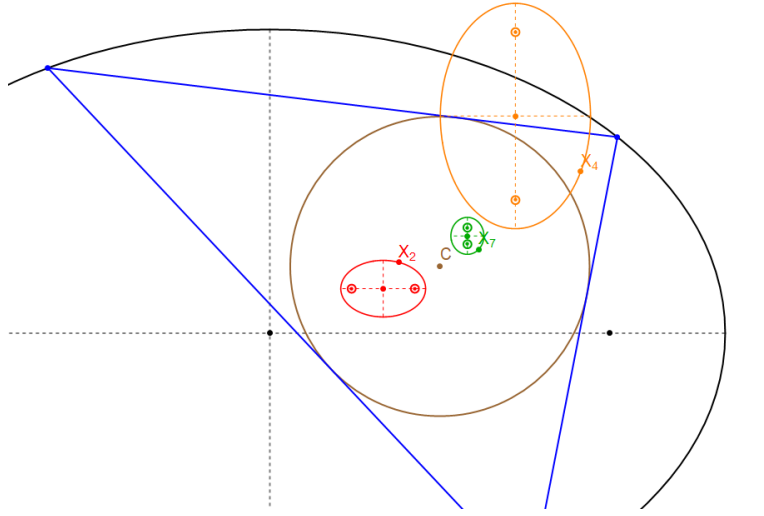


FIGURE 4. Close-up of the first quadrant of \mathcal{E} , showing a Poncelet triangle (blue) and the circular caustic centered on $C = X_1$. Also shown are the loci of the barycenter X_2 (red), orthocenter center X_4 (orange), and Gergonne point X_7 (green). [Video](#)

Note that $a_2/b_2 = a/b$, as claimed.

We note that this is a special case of [30, Thm.1], which states that for any pair of conics admitting a Poncelet family, the loci of both vertex and area centroids sweep conics. For triangles, these are coincident.

Referring to Figure 5, the following has been proved in [15]:

Theorem 3. Over \mathcal{T}_g the locus of X_4 is a conic homothetic to a 90° -rotated copy of \mathcal{E} . The locus center C_4 only depends on a, b of \mathcal{E} and C and is given by:

$$C_4 = \left[\frac{(a^2 + b^2)}{a^2} x_c, \frac{(a^2 + b^2)}{b^2} y_c \right]$$

Proposition 4. Over \mathcal{T} the semiaxis lengths a_4, b_4 of the X_4 locus are given by:

$$a_4^2 = \frac{z_4}{a^2 b^4 c^4}, \quad b_4^2 = \frac{z_4}{b^2 a^4 c^4}$$

where:

$$z_4 = (a^2 + b^2)(a^8 y_c^2 + b^8 x_c^2 - 4a^3 b^3 \delta) + a^8 b^4 + a^6 b^4 (6b^2 - z_4') + a^4 b^6 (b^2 - z_4')$$

$$z_4' = x_c^2 + y_c^2$$

Proof. CAS. Notice that $a_4/b_4 = a/b$. as required. \square

Let \mathcal{L}_7 denote the locus of the Gergonne point X_7 .

Proposition 5. Over \mathcal{T} , \mathcal{L}_7 is an ellipse with major (resp. minor) axis is parallel to \mathcal{E} 's minor (resp. major axis). The coordinates of its center $C_7 = [x_7, y_7]$ are given by:

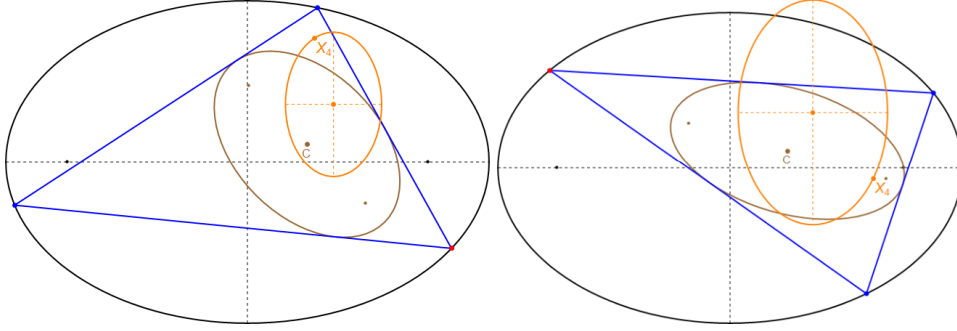


FIGURE 5. **left:** a Poncelet triangle (blue) interscribed between an outer ellipse \mathcal{E} and a generic caustic \mathcal{E}_c , let C be its center. Over the family, the locus of X_4 (orange) is homothetic to a 90° -rotated copy of \mathcal{E} . **right:** another caustic centered at C which closes Poncelet. Notice that the center of the (new) locus of X_4 remains at the same location. [Video](#)

$$x_7 = \frac{4ax_c(4a^5 + a^3b^2 + ab^4 - a(4a^2 - 3b^2)x_c^2 - ab^2y_c^2 - 3b\delta)}{a^2(4a^2 - b^2)^2 - (4a^2 - 3b^2)^2x_c^2 - a^2b^2y_c^2}$$

$$y_7 = \frac{4by_c(4b^5 + a^2b^3 + a^4b - b(4b^2 - 3a^2)y_c^2 - a^2bx_c^2 - 3a\delta)}{b^2(4b^2 - a^2)^2 - (3a^2 - 4b^2)^2y_c^2 - a^2b^2x_c^2}$$

Furthermore, the ratio of semi-axis lengths a_7/b_7 is given by:

$$\left(\frac{a_7}{b_7}\right)^2 = \frac{y_7 x_c}{x_7 y_c}$$

Proof. Symmetric parametrization yields an axis-aligned conic. \square

Observation 1. The semi-axis' lengths a_7, b_7 of \mathcal{L}_7 are rather long expressions, appearing in [Appendix D](#).

3.2. Loci of $\mathbf{X}(\mathbf{k})$, $\mathbf{k}=3,5,8$. The circumcenter X_3 is the center of the circumscribed circle. The Euler center X_5 is the center of the nine-point circle, which passes through the sides' midpoints. The Nagel point X_8 is the meet-point of lines from each vertex to where the opposite touches an excircle. For more information, see [37].

For the next three propositions, refer to [Figure 6](#). Let \mathcal{L}_3 be the (elliptic) locus of X_3 over \mathcal{T} .

Proposition 6. The foci F_3, F'_3 of \mathcal{L}_3 are collinear with C and are each railed to an axis of \mathcal{E} , namely:

$$F_3 = [x_c(1 - (b/a)^2), 0], \quad F'_3 = [0, y_c(1 - (a/b)^2)]$$

Furthermore, the locus semi-axis lengths a_3, b_3 of \mathcal{L}_3 are given by:

$$(2) \quad a_3 = \delta_3(a/b) - \delta'_3(b/a), \quad b_3 = \delta'_3 - \delta_3$$

where $\delta_3 = \frac{\sqrt{b^4 + c^2 y_c^2}}{2b}$ and $\delta'_3 = \frac{\sqrt{a^4 - c^2 x_c^2}}{2a}$.

Observation 2. In the special case when the circular caustic is concentric with \mathcal{E} , (i) $r = (ab)/(a+b)$, (ii) the invariant circumradius $R = (a+b)/2$, and (iii) X_3 sweeps a circle of radius $(a-b)/2$ concentric with \mathcal{E} [9, Section 3]. If the latter's center is thought of as two coinciding foci, note that each is still on an axis of \mathcal{E} , as required by [Proposition 6](#).

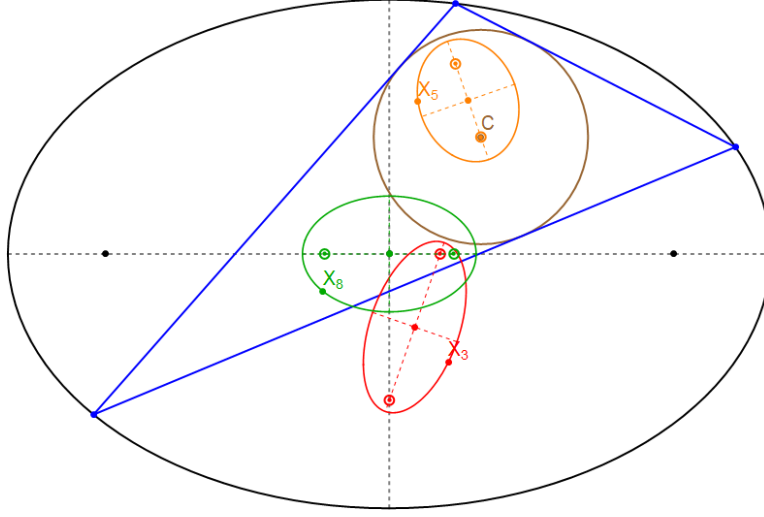


FIGURE 6. A Poncelet triangle (blue) is shown inscribed in an outer ellipse and circumscribing the incircle centered at $C = X_1$. Also shown are the loci of the circumcenter X_3 (red), Euler center X_5 (orange), and Nagel point X_8 (green). [Video 1](#), [Video 2](#)

Let \mathcal{L}_5 denote the (elliptic) locus of X_5 over \mathcal{T} .

Proposition 7. *Ae focus F'_5 of \mathcal{L}_5 is at $C = (x_c, y_c)$ and the other F'_5 is given by:*

$$F'_5 = \left[x_c \frac{1 + (b/a)^2}{2}, y_c \frac{1 + (a/b)^2}{2} \right]$$

Furthermore, the semi-axis lengths a_5, b_5 of \mathcal{L}_5 are given by:

$$a_5 = \frac{(a^5 + 3a^3b^2) \delta_3 - (b^5 + 3a^2b^3) \delta'_3}{abc^2}, \quad b_5 = \frac{(3a^3 + ab^2) \delta_3 - (3b^3 + a^2b) \delta'_3}{c^2}$$

where δ_3, δ'_3 are as defined for the locus of X_3 .

Proposition 8. *Over \mathcal{T} , the locus of the Nagel point X_8 is an ellipse homothetic and concentric with \mathcal{E} . Its semi-axis lengths a_8, b_8 are given by:*

$$a_8 = \frac{\sqrt{\delta_8}}{bc^2}, \quad b_8 = \frac{\sqrt{\delta_8}}{ac^2}$$

where: $\delta_8 = (a^3b + ab^3 - 2\delta)^2 + 4c^4x_c^2y_c^2$. Note that $a_8/b_8 = a/b$ as claimed.

Proof. Symmetric parametrization yields a concentric, axis-aligned conic. \square

3.3. Circular X(36). The inversive image of the incenter X_1 with the respect to the circumcircle is called X_{36} on [18]. Referring to Figure 7, the following is a rather surprising phenomenon:

Proposition 9. *Over \mathcal{T} , the locus of X_{36} is a circle. Its center C_{36} is given by:*

$$C_{36} = [x_{36}/z_1, y_{36}/z_1]$$

$$x_{36} = x_c (z_2 - 6a^4b^4 + 6a^4b^2y_c^2 - 3a^2b^6 - 2a^2b^4x_c^2 + 3a^2b^4y_c^2 - 8ab^3\delta + 3b^6x_c^2)$$

$$y_{36} = y_c (3a^6(y_c^2 - b^2) - a^4(6b^4 + b^2(2y_c^2 - 3x_c^2)) - 8a^3b\delta + a^2b^4(b^2 + 6x_c^2 - y_c^2) - 9b^6x_c^2)$$

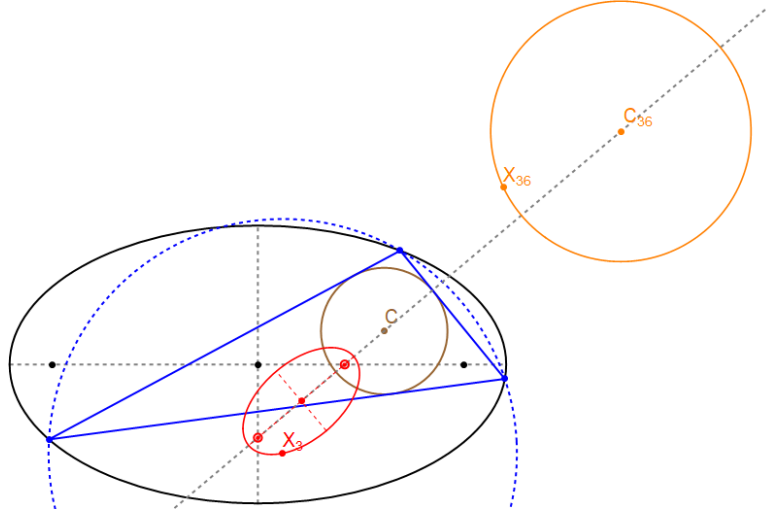


FIGURE 7. The locus of X_{36} , the inversion of $C = X_1$ (fixed) with respect to the (moving) circumcircle (dashed blue), is a circle (orange). Also shown is the elliptic locus of the circumcenter X_3 (red), whose foci F_3, F_3' lie on the semi-axes of the outer ellipse. Indeed, F_3, F_3', C, C_{36} are collinear. Note that from the inversion operation, $X_3 X_1 X_{36}$ are dynamically collinear. Indeed, the foci **live**

where:

$$\begin{aligned} z_1 &= z_2 - 2a^4b^4 - 6a^4b^2y_c^2 + a^2b^6 - 6a^2b^4x_c^2 - a^2b^4y_c^2 - 9b^6x_c^2 \\ z_2 &= a^6b^2 - 9a^6y_c^2 - a^4b^2x_c^2 \end{aligned}$$

Furthermore, the radius r_{36} of the locus X_{36} is given by:

$$\begin{aligned} r_{36} &= \frac{2(\delta_4 z_{36} - \delta_4' z_{36}')}{a^2b^2c^4 - b^2(a^2 + 3b^2)^2x_c^2 - a^2(3a^2 + b^2)^2y_c^2} \\ z_{36} &= 5ba^4y_c^2 - b^3a^2(a^2 + y_c^2 - x_c^2) + b^5(a^2 + 3x_c^2) \\ z_{36}' &= 5ab^4x_c^2 - a^3b^2(b^2 + x_c^2 - y_c^2) + a^5(b^2 + 3y_c^2) \end{aligned}$$

where $\delta_4 = \sqrt{a^4 - c^2x_c^2}$ and $\delta_4' = \sqrt{b^4 + c^2y_c^2}$.

Referring to Figure 8:

Proposition 10. *The major axis of \mathcal{L}_3 passes through the center C_{36} of the X_{36} locus. Furthermore, the circumradius is minimized (resp. maximized) when X_3 is on a major vertex of its locus closest (resp. farthest) from $C = X_1$. At these configurations, the distance $|X_1 X_{36}|$ maximized (resp. minimized), respectively.*

Proof. Direct from Proposition 6 and Proposition 9. \square

Referring to Figure 9:

Corollary 2. *Over \mathcal{T} , when C is at the center of \mathcal{E} , the locus of X_{36} is a circle concentric with \mathcal{E} , r_{36} reduces to:*

$$r_{36}^* = \frac{2ab}{a-b}$$

Proof. Direct from setting $x_c = y_c = 0$ in r_{36} (Proposition 9). \square

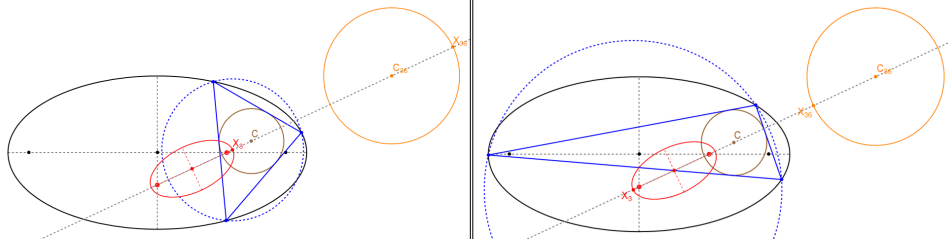


FIGURE 8. The major axis of the X_3 locus passes through the center C_{36} of the circular locus of X_{36} . On the left (resp. right), X_3 is at the major vertex of the locus closest to (resp. farthest from) $C = X_1$, in which case the circumradius is minimized (resp. maximized) and X_{36} is farthest from (resp. closest to) C . [live](#)

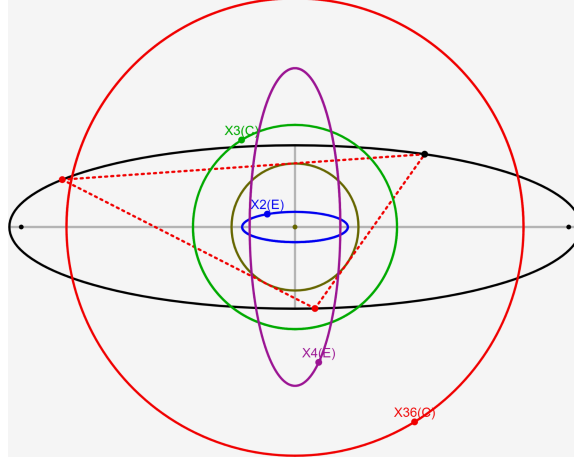


FIGURE 9. With $C = X_1 = [0, 0]$, the locus of X_{36} (red) is a circle concentric with \mathcal{E} . In the figure, $a = 7/2$ and $b = 1$, so $r_{36} = 14/5$. Also shown are the loci of X_2 (blue ellipse), X_3 (green circle) and X_4 (purple ellipse). [live](#)

4. DEGENERACIES

This section described many degeneracies brought about by the ‘presence’ of an equilateral triangle in \mathcal{T} . The locus of centroids of a 1d family of equilateral triangles inscribed in an ellipse $\mathcal{E} = (a, b)$ is an ellipse – henceforth called \mathcal{E}_{eq} – concentric and axis-aligned with \mathcal{E} , whose semi-axes a_{eq}, b_{eq} are given by [32, 34]:

$$a_{eq} = \frac{a c^2}{a^2 + 3b^2}, \quad b_{eq} = \frac{b c^2}{3a^2 + b^2}.$$

Let \mathcal{T}^* denote the family of Poncelet triangles about a circle with center $C = [a_{eq} \cos t, b_{eq} \sin t]$ on \mathcal{E}_{eq} .

Corollary 3. \mathcal{T}^* contains an equilateral triangle.

Let $V^* = [a \cos(t^*), b \sin(t^*)]$ on \mathcal{E} be a vertex of said equilateral.

Proposition 11. t^* is given by the three solutions of:

$$\begin{aligned} & (a^2 + 3b^2) [(3a^2 + b^2) \cos^2 t^* - 2b^2 \sin^2 t - 2b^2 \sin t \sin t^*] \\ & + (3a^2 + b^2) [-2a^2 \cos t \cos t^* + (a^2 - 3b^2) \cos^2 t] = 0 \end{aligned}$$

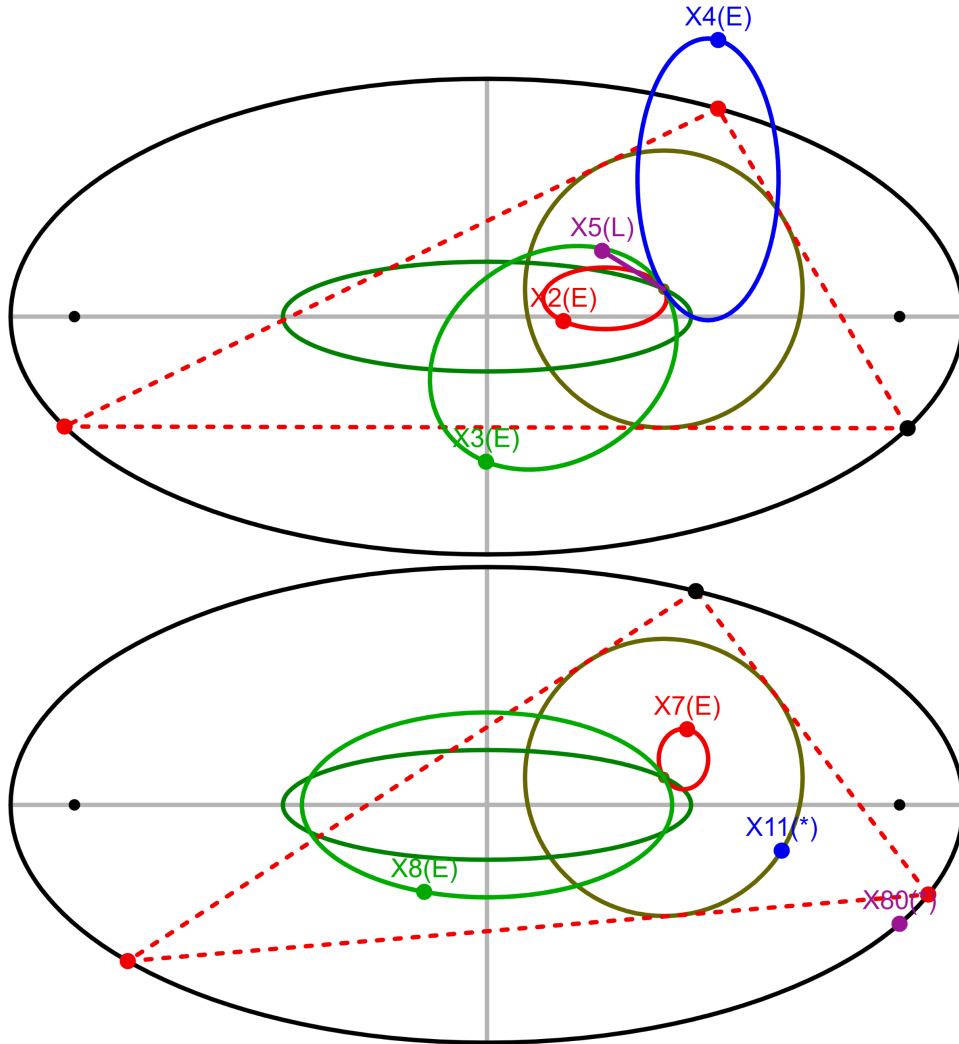


FIGURE 10. **top**: when the incenter is on \mathcal{E}_{eq} (dark green), the loci of X_k , $k = 2, 3, 4, 5$ (red, light green, blue, purple), pass simultaneously through the incenter when the equilateral in the family is traversed, notice that the locus of X_5 (purple) has collapsed to a segment, **live**; **bottom**: same situation, showing the loci of X_k , $k = 7, 8, 11, 80$ (red, light green, blue, purple). The latter two are stationary on the incircle and \mathcal{E} , respectively, and along the X_1X_5 line, **live**

Proof. It can be shown that a triangular orbit will be equilateral when the triangle $\{V^*, C, [a \cos t, -b \sin t]\}$ is isosceles. \square

Sample loci of X_k , $k = 2, 3, 4, 5$ over \mathcal{T}^* are shown Figure 10 (top). Notice they simultaneously pass through X_1 when the Poncelet triangle becomes an equilateral. In Figure 10 (bottom) are shown the loci of $k = 7, 8, 11, 80$. The first two display the same behavior, while the latter two are stationary.

4.1. **C is a vertex of X(3).** Referring to Figures 11 and 12:

Corollary 4. *Over \mathcal{T}^* C is a (major) vertex of \mathcal{L}_3 . If C is interior (resp. exterior) to \mathcal{E}_{eq} , it is interior (resp. exterior) to \mathcal{L}_3 .*

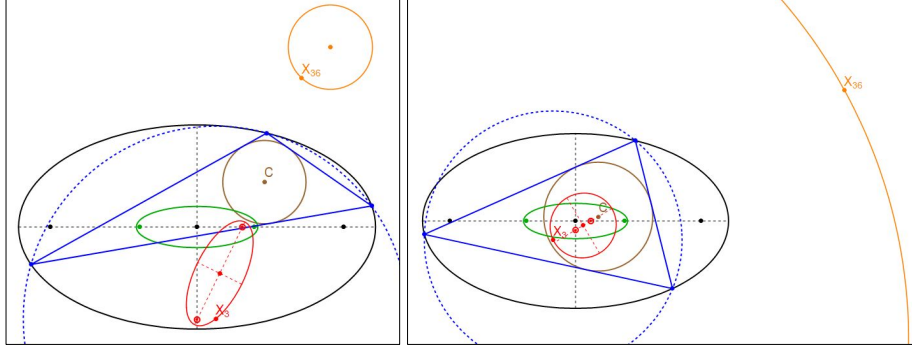


FIGURE 11. On the left (resp. right), $C = X_1$ is outside (resp. inside) \mathcal{E}_{eq} (green). In this case, C is exterior (resp. interior) to the locus of X_3 (red), and the locus of X_{36} (orange) is disjoint with (resp. contains) \mathcal{E} .

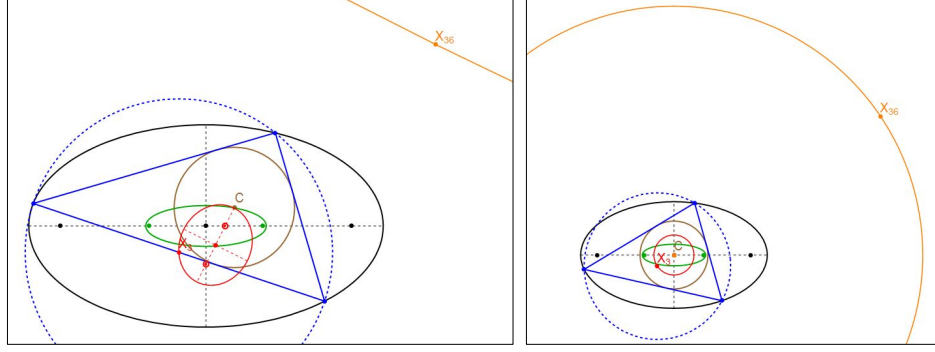


FIGURE 12. On the left (resp. right), $C = X_1$ is on (resp. at the center of) \mathcal{E}_{eq} (green). In this case, C is a vertex (at the center) of the locus of X_3 (red), and the locus of X_{36} (orange) is a line (resp. a circle concentric with \mathcal{E}).

Proof. This stems from the fact that the major axis of the X_3 locus passes through C , [Proposition 6](#). \square

4.2. Invariant eccentricity: $\mathbf{X}(3)$, $\mathbf{X}(7)$.

Proposition 12. *Over all C on \mathcal{E}_{eq} the aspect ratio of \mathcal{L}_3 is invariant and given by:*

$$\frac{a_3}{b_3} = \frac{(3a^2 + b^2)(a^2 + 3b^2)(a^4 - b^4)}{c^2(6a^5b + 20a^3b^3 + 6ab^5)}$$

Proof. Evaluating [Equation \(2\)](#) over [Proposition 17](#). \square

Proposition 13. *Over all C on \mathcal{E}_{eq} , the aspect ratio \mathcal{L}_7 is invariant and given by:*

$$\frac{a_7}{b_7} = \frac{2a^2 + b^2}{\sqrt{2a^4 + 5a^2b^2 + 2b^4}}$$

Proof. Direct from [Proposition 5](#). \square

4.3. Segment X(5).

Proposition 14. *Over all $C = [a_{eq} \cos t, b_{eq} \sin t]$ on \mathcal{E}_{eq} , \mathcal{L}_5 is a segment ($b_5 = 0$) of length l_5 with an endpoint on C and the other at $F'_{5,eq}$. These are given by:*

$$l_5^2 = \frac{c^8 (a^6 + 15a^4b^2 + 15a^2b^4 + b^6 - c^6 \cos(2t))}{16 (3a^5b + 10a^3b^3 + 3ab^5)^2}$$

$$F'_{5,eq} = \left[\frac{(a^4 - b^4) \cos t}{2(a^3 + 3ab^2)}, \frac{(a^4 - b^4) \sin t}{2(3a^2b + b^3)} \right]$$

Proof. Applying Proposition 7 on Proposition 17. \square

Corollary 5. *Over \mathcal{T}^* the locus of X_{12} (internal center of similitude of the incircle and the Euler circle [18]), is a segment with one endpoint at C .*

Proof. This must be the case because the segment locus of the Euler center X_5 passes through C . \square

4.4. Stationary X(11), X(80). Referring to Figure 19:

Proposition 15. *Over \mathcal{T}^* , the Feuerbach point X_{11} (resp. X_{80} , the reflection of X_1 on X_{11}) is stationary at the non- C intersection of the segment-locus of X_5 with the incircle (resp. with \mathcal{E}). With $C = [a_{eq} \cos t, b_{eq} \sin t]$ on \mathcal{E}_{eq} , these are given by:*

$$X_{11}^* = \frac{a^2 + b^2}{c^2} [a_{eq} \cos t, -b_{eq} \sin t]$$

$$X_{80}^* = [a \cos t, -b \sin t]$$

Note that $X_k, k = 1, 5, 11, 12, 80, \dots$, are points on the X_1X_5 line [19].

Proof. CAS manipulation. \square

Observation 3. *Over \mathcal{T}^* , the locus of X_{106} (isog. conj. of X_1X_2 with the line at infinity) is a circle passing through X_{80} .*

Lemma 1. *Let $C = [a_{eq} \cos t, b_{eq} \sin t]$. Over \mathcal{T}^* , the intersection $I^* = [x^*, y^*]$ of the ray X_1X_5 with \mathcal{E} is given by:*

$$x^* = \frac{(a^2v (a^4 - 3a^2b^2 - 2b^4) \sin^2 t - b^4u^2 \cos^2 t) a \cos t}{b^4u^2 \cos^2 t + a^4v^2 \sin^2 t}$$

$$y^* = \frac{(b^2u (2a^4 + 3a^2b^2 - b^4) \cos^2 t + a^4v^2 \sin^2 t) b \sin t}{b^4u^2 \cos^2 t + a^4v^2 \sin^2 t}$$

where $u = (3a^2 + b^2)$ and $v = (3b^2 + a^2)$.

Referring to Figure 13:

Proposition 16. *In \mathcal{T}^* , the Poncelet triangle $I^*B_1B_2$ is an isosceles, unique in the family (other than the equilateral), with base B_1B_2 , the chord of \mathcal{E} tangent to the incircle at the stationary X_{11} .*

Proof. The triangle is an isosceles since I^*, X_1, X_5 are collinear. The base must be tangent to the incircle (via Poncelet) at X_{11} , since the latter is collinear with X_1 and X_5 [18]. We omit the expressions for B_1 and B_2 since they are rather long. \square

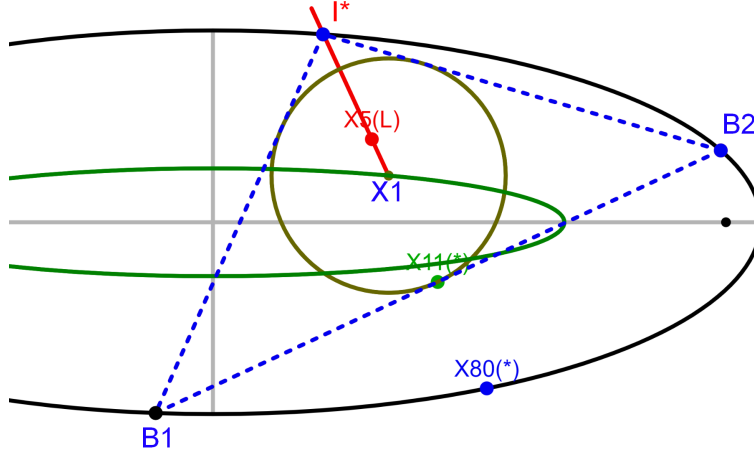


FIGURE 13. Construction for Proposition 16: $C = X_1$ on \mathcal{E}_{eq} , the Poncelet triangle has a vertex on the intersection I^* of the ray X_1X_5 with \mathcal{E} . The said triangle is an isosceles, and its base B_1B_2 is the chord of \mathcal{E} touching the incircle at X_{11} . *live*

4.5. **Line X(36).** In Proposition 9 we saw that over \mathcal{T} , the locus X_{36} was a circle. Nevertheless, and referring to Figure 12 (left):

Proposition 17. *Over \mathcal{T}^* , with $C = [x_c, y_c]$ on \mathcal{E}_{eq} , the locus of X_{36} degenerates to the line:*

$$b^2x_cx + a^2y_cy = \frac{b^2(a^4 + 2a^2b^2 + 5b^4)x_c^2 + a^2(5a^4 + 2a^2b^2 + b^4)y_c^2}{c^4}$$

Proof. Direct from Proposition 9, taking the limit when (x_c, y_c) is on \mathcal{E}_{eq} and simplifying. \square

Referring to Figure 11:

Observation 4. *Over \mathcal{T}^* , the locus of X_{36} is disjoint with (resp. contains) \mathcal{E} if C is exterior (resp. interior) to \mathcal{E}_{eq} .*

Referring to Figure 14:

Proposition 18. *If $C = [x_c, y_c]$ is on \mathcal{E}_{eq} , the major axis of \mathcal{L}_3 is perpendicular to the line locus of X_{36} . These meet at:*

$$X_{36}^\perp = c^{-4} [x_c(a^4 + 2a^2b^2 + 5b^4), y_c(b^4 + 2b^2a^2 + 5a^4)]$$

Proof. Direct from Proposition 6 which the X_3 -locus major axis, and Proposition 17. \square

Observation 5. *Over \mathcal{T}^* , when X_3 passes through $C = X_1$, i.e., the major vertex of its locus, X_{36} is on the line at infinity.*

Referring to Figure 15, we specialize Proposition 10 to its degenerate form:

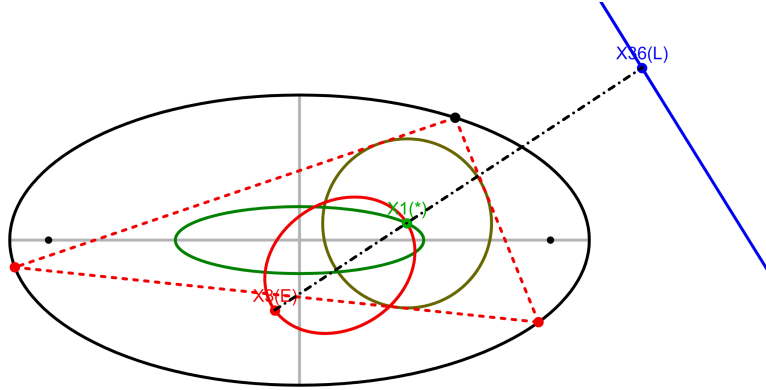


FIGURE 14. When X_3 is on the non- X_1 major vertex of its locus (red), X_3X_1 is perpendicular to the line-locus of X_{36} . At this moment, $|X_1X_{36}|$ is minimal. *live*

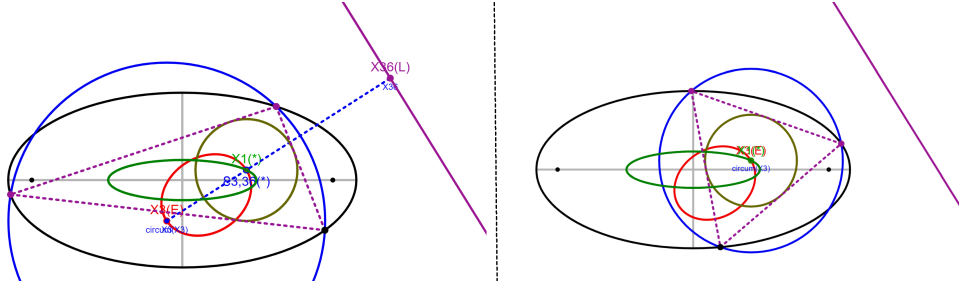


FIGURE 15. **left:** When X_3 is on the non- X_1 vertex of its locus, the circumradius R is maximized and $|X_1X_{36}|$ is minimal; **right:** if X_3 on X_1 , the triangle is equilateral, R is minimized while $|X_1X_{36}|$ is 'maximal', since X_{36} is on the line at infinity. *live*

Proposition 19. *Over \mathcal{T}^* , when X_3 is on the non- X_1 major vertex of its locus, the distance $|X_1X_{36}|$ is minimal and given by:*

$$|X_1X_{36}|_{min} = \frac{4(a^2 + b^2) \sqrt{a^4y_c^2 + b^4x_c^2}}{c^4}$$

Furthermore, the circumradius R is minimized (resp. maximized) when $X_3 = X_1$ (resp. X_3 is on the non- X_1 vertex of its locus).

$$R_{min} = 2 \left(\frac{b\sqrt{a^4 - c^2x_c^2} - a\sqrt{b^4 + c^2y_c^2}}{c^2} \right)$$

$$R_{max} = \frac{(a^2 + b^2) \sqrt{a^4 + 6a^2b^2 + b^4} \sqrt{a^4y_c^2 + b^4x_c^2}}{2a^2b^2c^2}$$

Referring to Figure 16:

Observation 6. *Over all C on \mathcal{E}_{eq} , the envelope of the line locus of X_{36} is an oval of degree 6.*

4.6. Elliptic X(59). Referring to Figure 17, in several Poncelet families studied, the locus of X_{59} , the isogonal conjugate of X_{11} , is either an oval or a self-intersected curve, e.g., see [11, Fig.2] and [26, Fig.9].

Nevertheless, it collapses to a conic in the following two cases. Firstly:

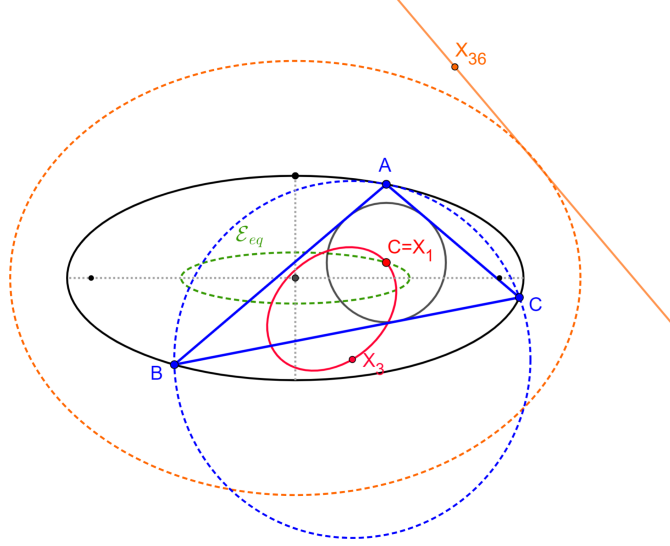


FIGURE 16. Over all $C = X_1$ on \mathcal{E}_{eq} (dashed green), the envelope of the line locus of X_{36} is a non-conic of degree 6 (dashed orange).

Proposition 20. *In Chapple's porism, the locus of X_{59} is an ellipse with major axis on X_1X_3 , with semi-axis lengths given by:*

$$a_{59, \text{chapple}} = R, \quad b_{59, \text{chapple}} = \frac{R\sqrt{R^2 - d^2}}{\sqrt{9R^2 - d^2}}$$

The *isogonal conjugate* $g(P)$ of a point P with respect to a triangle T is the point of concurrence of the cevians of P reflected upon the angle bisectors [37]. In [33] it is shown that the locus of $g(P)$ over circle-inscribed Poncelet triangles is a circle. As above, let \mathcal{T}_g be a family of Poncelet triangles interscribed between two generic conics $\mathcal{E}, \mathcal{E}_c$. Referring to Figure 18, the following is proved in [10]:

Lemma 2. *Over \mathcal{T}_g , the locus of $g(P)$ is a conic. If P is on \mathcal{E}_c the locus is an ellipse interior to \mathcal{E} and touching it at a point. If P is on \mathcal{E} the locus is the union of a straight line and the line at infinity (degenerate hyperbola).*

An alternative proof to Proposition 17 is to be based on the fact that X_{36} and X_{80} are isogonal conjugates [18]:

Corollary 6. *Over \mathcal{T}^* , the locus of X_{36} is a line since X_{80} is stationary on \mathcal{E} , Proposition 15.*

Secondly, referring to Figure 17 (bottom right) and Figure 19:

Corollary 7. *Over \mathcal{T}^* , the locus of X_{59} is an ellipse interior to \mathcal{E} and touching it at a point.*

Proof. X_{59} is the isogonal conjugate of X_{11} [18], which is stationary on the incircle over \mathcal{T}^* . \square

Furthermore, let I^* denote the touch-point between the elliptic locus of X_{59} (over \mathcal{T}^*) and \mathcal{E} .

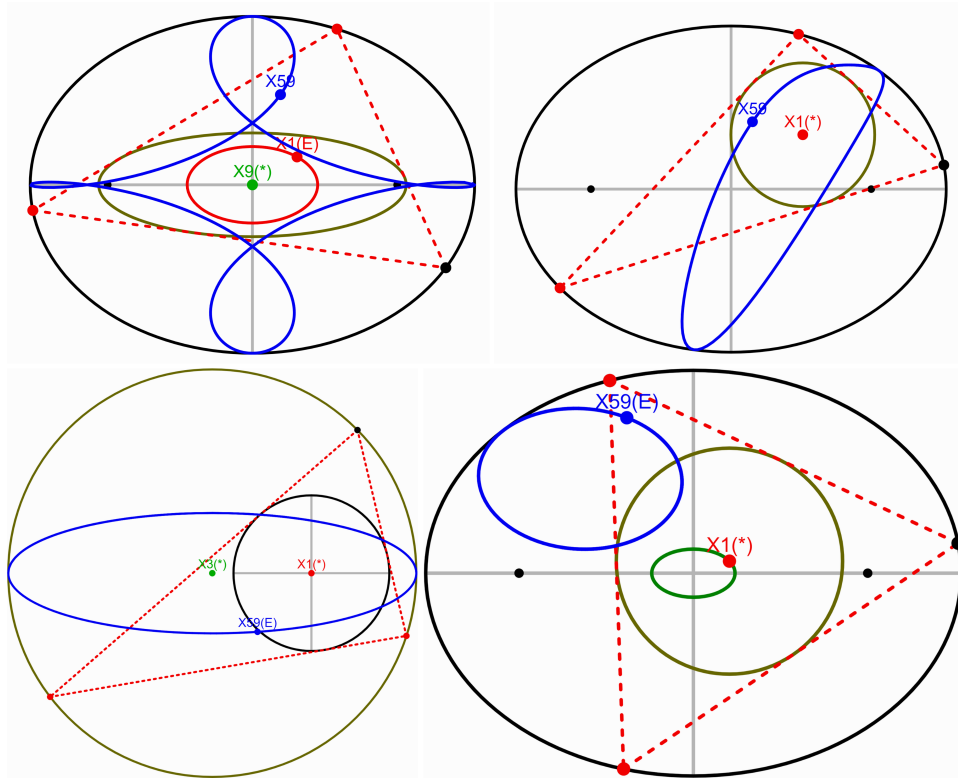


FIGURE 17. The locus of X_{59} (isogonal conjugate of X_1 in (i) the confocal pair (top left), (ii) a generic incircle porism (top right), (iii) Chapple's porism, where it is an ellipse (top bottom), and (iv) an incircle porism with X_1 on \mathcal{E}_{eq} (dark green), notice X_{59} is a conic, tilted with respect to \mathcal{E} , which it touches at a single point.

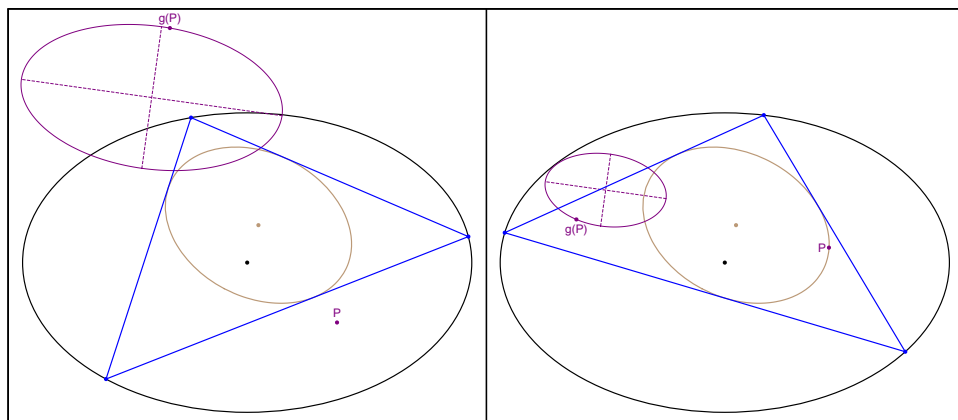


FIGURE 18. Results from [10]: **left**: over generic Poncelet triangles, the locus of the isogonal conjugate $g(P)$ of a fixed point P is a conic (purple); **right**: if P is on the caustic, the locus of $g(P)$ is an ellipse that touches \mathcal{E} at one point. [Video](#)

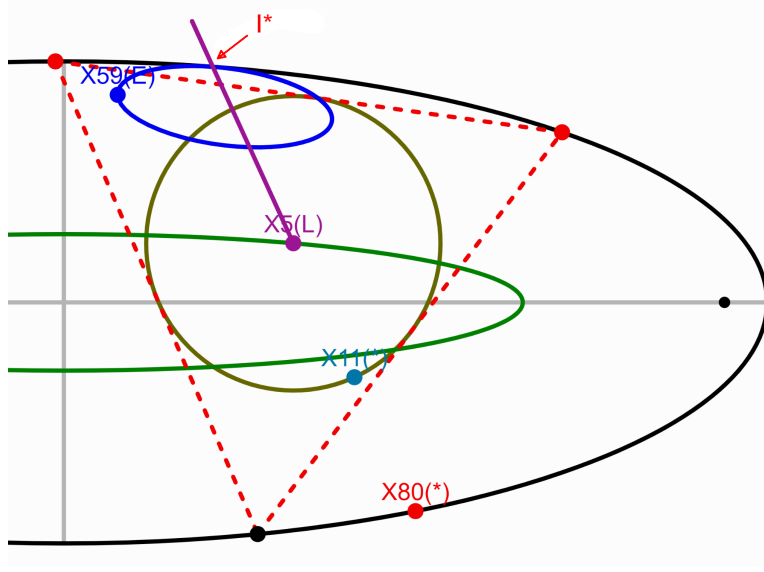


FIGURE 19. When the incenter is on \mathcal{E}_{eq} (dark green), the locus of X_5 is a line, and X_{11} and X_{80} are stationary on the incircle and \mathcal{E} , respectively. The locus of X_{59} is an ellipse (blue), internally-tangent to \mathcal{E} at I^* (see Lemma 1) In the picture, X_5 is on X_1 , i.e., the Poncelet triangle is an instantaneous equilateral. When this happens, X_{59} is at a vertex of its locus. **live**

Observation 7. *When the Poncelet triangle is an isosceles, i.e., one of its vertices is I^* , X_{59} is at I^* . When the Poncelet triangle is an equilateral, X_{59} ‘blows up’ at a major vertex of its locus.*

5. ENVELOPES

As before, let \mathcal{T} be a family of Poncelet triangles inscribed in an ellipse \mathcal{E} and circumscribing a circle \mathcal{K} with center $C = X_1$.

5.1. **Circumcircle.** Referring to Figure 20:

Proposition 21. *Over \mathcal{T} , the envelope of the circumcircle are two nested circles, each tangent to \mathcal{E} at two points and centered at the foci F_3 and F'_3 of X_3 locus (Proposition 6).*

Proof. Let $C = (x_c, y_c)$ be the center of caustic and r the radius of the caustic given by Proposition 2; the incircle \mathcal{K} is then given by $(x - x_c)^2 + (y - y_c)^2 = r^2$. Let $\lambda = \cos u + i \sin u$ in the symmetric parametrization of Section 2.2, obtain the circumcircle \mathcal{K}' :

$$\begin{aligned} \mathcal{K}'(x, y) = & x^2 + y^2 - \left(\frac{(a^3 b - \delta) \cos u}{b a^2} + \frac{c^2 y_c x_c \sin u}{b a^2} + \frac{c^2 x_c}{a^2} \right) x \\ & + \left(-\frac{c^2 x_c y_c \cos u}{a b^2} + \frac{c^2 y_c}{b^2} + \frac{(a b^3 - \delta) \sin u}{a b^2} \right) y + \frac{c^2 x_c \cos u}{a} + \frac{c^2 y_c \sin u}{b} - \frac{\delta}{ba} = 0 \end{aligned}$$

The envelope of this family of circles is obtained by setting:

$$\mathcal{K}'(x, y) = 0, (\partial \mathcal{K}' / \partial u)(x, y) = 0$$

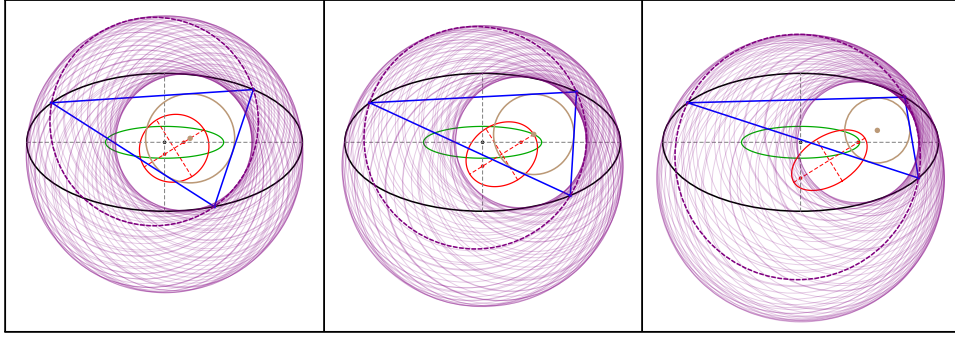


FIGURE 20. The envelope of the circumcircle consists of two nested circles twice tangent to \mathcal{E} and centered on the foci of the X_3 locus (red). Left, middle, right show three positions for $C = X_1$: interior, on the boundary, and exterior to \mathcal{E}_{eq} (green), respectively. [Video](#)

With the above equations this yields the union of two circles $\mathcal{K}_1 = (O_1, r_1)$ and $\mathcal{K}_2 = (O_2, r_2)$ where:

$$\begin{aligned} O_1 &= [0, -y_c c^2 / b^2] = [0, y_c(1 - (a/b)^2)] = F'_3 \\ r_1 &= (a/b^2) \sqrt{b^4 + c^2 y_c^2} \\ O_2 &= [x_c c^2 / a^2, 0] = [x_c(1 - (b/a)^2), 0] = F_3 \\ r_2 &= (b/a^2) \sqrt{a^4 - c^2 x_c^2} \end{aligned}$$

\mathcal{K}_1 touches \mathcal{E} at $[\pm(a/b)\sqrt{b^2 - y_c^2}, y_c]$; \mathcal{K}_2 touches \mathcal{E} at $[x_c, \pm(b/a)\sqrt{a^2 - x_c^2}]$. \square

Given two fixed nested (resp. unnested) circles, the locus of the center of circles simultaneously tangent to them is a conic with foci on their centers and with major axis length equal to the difference (resp. sum) of their radii [22, thm.14, p.57]. In our case, the circumcircles of a Poncelet family circumscribing a circle are tangent to the two circular boundaries of their envelope. In Equation (2), an expression is derived for a_3 , the semi-axis length of the locus of X_3 . It follows that:

Corollary 8. $|r_1 - r_2| = 2a_3$.

For the general case, experimental evidence suggests:

Conjecture 1. *Over \mathcal{T}_g , either component of the envelope of the circumcircle is a conic if and only if \mathcal{E}_c is a circle, in which case both components are circles (Proposition 21).*

Note that if the outer conic is a circle, said envelope is not defined.

5.2. Radical axis. Let \mathcal{R} denote the radical axis of incircle and circumcircle of a triangle, i.e., the line whose points have equal circle power with respect to the two said circles [37]. $X_1 X_3$ must be perpendicular to \mathcal{R} since it is the line that passes through both circle centers. According to [18], X_{3660} is the ‘trace’ of \mathcal{R} , i.e., the perpendicular intersection of $X_1 X_3$ with the radical axis.

Referring to Figure 21:

Proposition 22. *Over \mathcal{T} , the envelope of \mathcal{R} is a conic whose major axis coincides with that of the X_3 locus (see Proposition 6). It will be an ellipse (resp. hyperbola) if C is interior (resp. exterior) to \mathcal{E}_{eq} .*

Proof. Let $C = (x_c, y_c)$ be the center of caustic and r the radius of the caustic given by [Proposition 2](#); the incircle \mathcal{K} is then given by $(x - x_c)^2 + (y - y_c)^2 = r^2$. Let $\lambda = \cos u + i \sin u$ in the symmetric parametrization of [Section 2.2](#), obtain the circumcircle \mathcal{K}' :

$$\begin{aligned} \mathcal{K}'(x, y) = & x^2 + y^2 - \left(\frac{(a^3b - \delta)}{b a^2} \cos u + \frac{c^2 y_c x_c}{b a^2} \sin u + \frac{c^2 x_c}{a^2} \right) x \\ & + \left(-\frac{c^2 x_c y_c}{a b^2} \cos u + \frac{(a b^3 - \delta)}{a b^2} \sin u + \frac{c^2 y_c}{b^2} \right) y + \frac{c^2 x_c}{a} \cos u + \frac{c^2 y_c}{b} \sin u - \frac{\delta}{ba} = 0 \end{aligned}$$

The radical axis of (K, \mathcal{K}') , is given by $l(u)x + m(u)y + n(u) = 0$, with:

$$\begin{aligned} l(u) &= c^4 (-b x_c y_c c^2 \sin u + b (\delta - a^3 b) \cos u + b^2 (a^2 + b^2) x_c) \\ m(u) &= c^4 (a (a b^3 - \delta) \sin u - a x_c y_c c^2 \cos u + a^2 (a^2 + b^2) y_c) \\ n(u) &= a^2 b y_c c^6 \sin u + a b^2 x_c c^6 \cos u + a^2 b^2 c^2 (-a^2 x_c^2 + b^2 y_c^2) + a^4 b^4 (a^2 + b^2) \\ &\quad - ab (a^4 + b^4) \delta. \end{aligned}$$

The envelope of the family of lines above is given by:

$$E(u) = \left[\frac{n'(u)m(u) - m'(u)n(u)}{m'(u)l(u) - l'(u)m(u)}, -\frac{n'(u)l(u) - l'(u)n(u)}{m'(u)l(u) - l'(u)m(u)} \right]$$

It follows from the calculations that the envelope is parametrized by:

$$E(u) = \left[\frac{k_1 \sin u + k_2 \cos u + k_3}{d_1 \sin u + d_2 \cos u + d_3}, \frac{m_1 \sin u + m_2 \cos u + m_3}{d_1 \sin u + d_2 \cos u + d_3} \right]$$

Here all constants are long expressions involving the variables (a, b, c, x_c, y_c) . Eliminating the variables we obtain that the envelope is given implicitly by a quadratic equation and so it is a conic. Algebraic manipulation yields its major axis to be as the one in [Proposition 6](#). \square

Referring to [Figure 22](#):

Corollary 9. *Over \mathcal{T} , the envelope of \mathcal{R} is a parabola if C is on the boundary of \mathcal{E}_{eq} whose axis of symmetry is the major axis of the X_3 locus, i.e., its directrix is parallel to the line-locus of X_{36} ([Proposition 17](#)).*

Proof. When the family is at the equilateral position, X_1 and X_3 coincide, and \mathcal{R} is the line at infinity. \square

Based on experimental evidence:

Conjecture 2. *Over \mathcal{T} , the envelope of \mathcal{R} is a conic if and only if the Poncelet caustic is a circle.*

The Feuerbach point X_{11} is where incircle and nine-point circle touch. Therefore, the radical axis of said circles is tangent to the incircle at X_{11} . Let said axis be called $L(101)$ after [\[37\]](#). Therefore:

Corollary 10. *Over \mathcal{T} , the envelope of $L(101)$ is the incircle itself. If C is on \mathcal{E}_{eq} , X_{11} is stationary ([Proposition 15](#)), therefore, in such a case said envelope is undefined.*

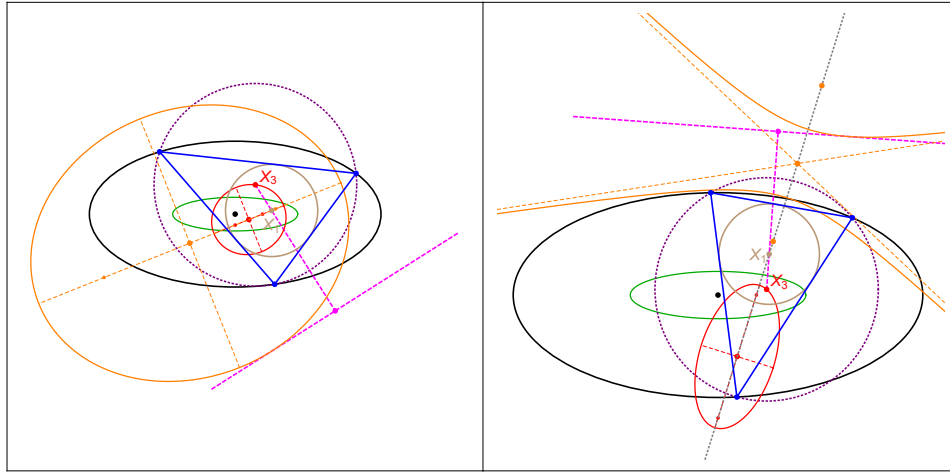


FIGURE 21. Left (resp. right): envelope (orange) of \mathcal{R} (dashed magenta) is an ellipse (resp. hyperbola), when $C = X_1$ is interior (resp. exterior) to \mathcal{E}_{eq} (green ellipse). The major axis of the locus of X_3 (red) coincides with that of the envelopes.

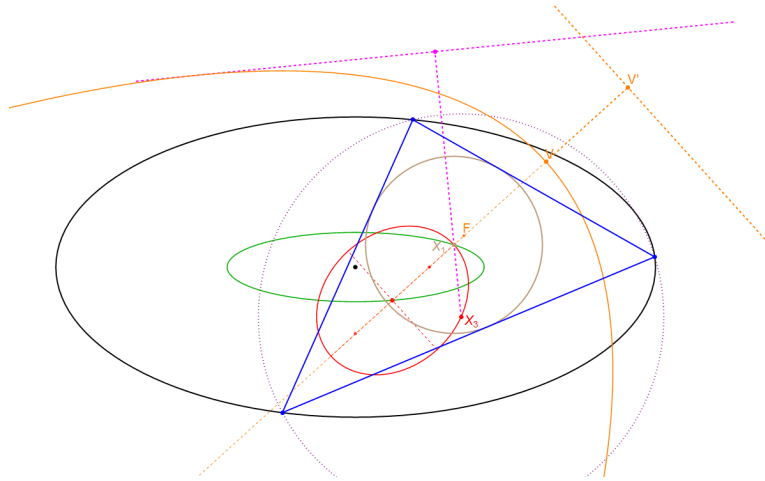


FIGURE 22. When $C = X_1$ is on the boundary of \mathcal{E}_{eq} (green ellipse), the envelope of \mathcal{R} (dashed magenta) is parabolic (orange, focus F , vertex V); the axis of symmetry (dashed orange) is the major axis of the locus of X_3 (red). Also shown is the directrix of the parabola (dashed orange), with V' its intersection with the axis of symmetry.

The *orthic axis*, called \mathcal{L}_3 in [37] (resp. *anti-orthic axis*, \mathcal{L}_1) is the radical axis of the circumcircle and the nine-point (resp. Bevan) circle [37, Radical line], the latter is centered on X_5 (resp. X_{40}) and has radius $R/2$ (resp. $2R$). Experimentation shows:

Observation 8. *Over \mathcal{T} , the envelope of both \mathcal{L}_3 and \mathcal{L}_1 are conics: an (ellipse, parabola, hyperbola) if C is (interior, on the boundary, exterior) to E_{eq} respectively. Nevertheless, the envelope axes and those of the X_3 locus are not axis-aligned.*

Family	Outer	Inner	X_1	X_7	X_8	bit.ly/<code>
Confocal	E	E	E	E	E	46KYk4D
Chapple	C	C	P	C	C	4cqyGmN
Incircle	E	C	P	E	E	3M50bHG
Circ-caustic	E	C	P	E	E	4fK8Exy
Homothetic	E	E	-	-	-	3M4sG8G
Dual	E	E	-	-	-	3WHkQqg
Conf. Excentrals	E	E	-	-	-	3WGARgk
Inellipse	C	E	-	-	-	4fKZPUv
Brocard	C	E	-	-	-	4fKQmMH
MacBeath	C	E	-	-	-	3M3xtaj

TABLE 1. The loci of $X_k, k = 1, 7, 8$ for 10 Poncelet conic configurations. ‘Inner’ and ‘Outer’ indicate if such conics are either ellipses (E) or circles (C). Under columns labeled X_k ($k = 1, 7, 8$), symbols ‘E’, ‘C’, ‘P’, ‘-’ indicate if the corresponding locus is an ellipse, a circle, a point, or a non-conic, respectively. The pattern that emerges is that X_7 and X_8 can only be conics if ‘Inner’ is a circle, in which case X_1 is a point. The confocal family is one exception: the inner conic is a (confocal) ellipse, and all three centers sweep conics. Note: the last column gives a hyperlink to an animated view of the family.

6. ELLIPTICITY OF $X(k), k=1, 7, 8$

In [11, 29] it is proved that the locus of the incenter X_1 is a conic if the Poncelet ellipse pair is confocal (elliptic billiard). In [16, Conj.3] it is conjectured that X_1 sweeps a conic if and only if the pair is confocal, and a proof is still outstanding.

Experiments with ten different Poncelet families (see six of them in Figures 23 and 24) are summarized in Table 1. In turn, these suggest:

Conjecture 3. *The locus of X_7 and/or X_8 are conics if and only if (i) the Poncelet conic pair is confocal or (ii) the caustic is a circle (in which case X_1 is stationary).*

Note that for the case of the bicentric pair, the locus of both X_7 and X_8 are circles [21].

7. FOUR SPECIAL FAMILIES

We study four special families of ellipse-inscribed Poncelet triangles about the incircle. Referring to Figure 25, these are: (i) focal- X_1 : the caustic is centered on a focus of E ; (ii) iso- X_2 : caustic is on a first special point such that the barycenter X_2 is stationary; (iii) focal- X_4 : caustic is centered on a second special point such that the orthocenter X_4 is stationary on a focus of E ; (iv) iso- X_7 : caustic is centered on a third special point such that the Gergonne point X_7 is stationary.

In the calculations below, $R, r, l_i, i = 1, 2, 3$ refer to a triangle’s circumradius, inradius, and sidelengths, respectively.

7.1. **Focal- $X(1)$.** Referring to Figure 25 (top left):

Proposition 23. *The caustic centered at $C_1 = [c, 0]$ closes Poncelet $N = 3$ with radius r_1 given by:*

$$r_1 = \frac{b^2}{c^2} \left(\sqrt{a^2 + c^2} - a \right)$$

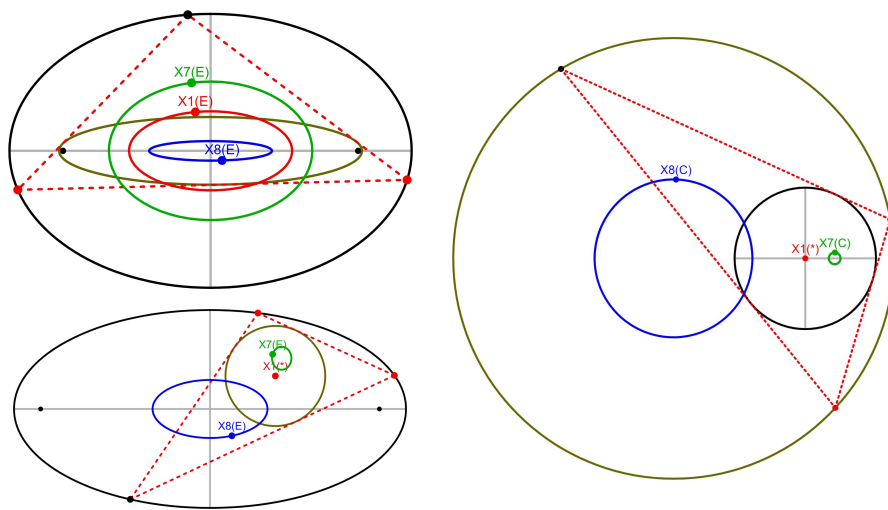


FIGURE 23. Three Poncelet families for which the loci of X_k , $k = 1, 7, 8$ are conics: (i) **top left**: confocal pair, **live**; (ii) **bottom left**: generic circular caustic, **live**; (iii) **right**: Chapple's porism (bicentric $n = 3$), **live**. Note that in (ii) and (iii), X_1 is stationary (center of caustic). Also note that in (iii), the loci of X_7 and X_8 are circles.

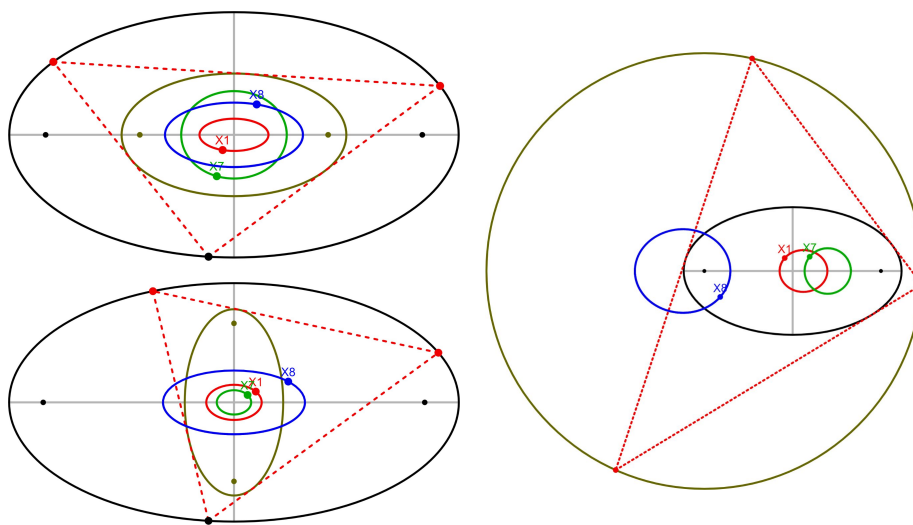


FIGURE 24. Three Poncelet families for which the loci of X_k , $k = 1, 7, 8$ are non-conics: (i) **top left**: pair of homothetic ellipses, **live**; **bottom left**: pair of 'dual' ellipses, **live**; (iii) **right**: the MacBeath family, **live**.

Proof. Direct from Proposition 2.

□

Observation 9. *The focal- X_1 family is the polar image of the vertices of Chapple's Porism (a porism of triangles interscribed between two circles [21]), with respect to*

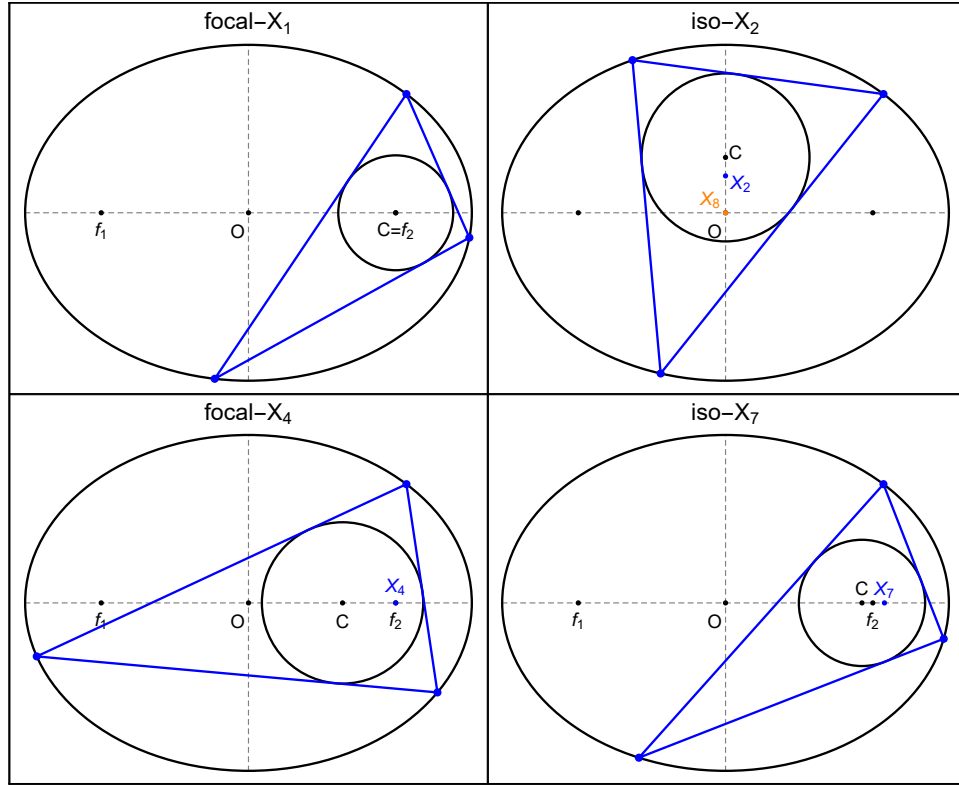


FIGURE 25. Four families of ellipse-inscribed Poncelet triangles about the incircle: focal- X_1 (top left); iso- X_2 (top right); focal- X_4 (bottom left); iso- X_7 (bottom right). [Video](#)

the circumcircle, i.e., it is its tangential triangle. The former's X_1 coincides with the latter's circumcenter X_3 .

While bicentric n -gons (a generalization of Chapple's porism) conserve the sum of cosines [28], their polar family conserve $\sum_{i=1}^n \sin(\theta_i/2)$, for all $n \geq 3$ [2, prop.26].

Proposition 24. For the focal- X_1 family, the invariant sum of half-angle sines is given by:

$$\sum_{i=1}^3 \sin \frac{\theta_i}{2} = \frac{c^2 - a^2 + a\sqrt{a^2 + c^2}}{c^2}$$

7.2. **Iso- $X(2)$.** Referring to Figure 25 (top right):

Proposition 25. For a circular caustic with center and radius given by:

$$C_2 = \left[0, \frac{cb}{2a} \right], \quad r_2 = \frac{b}{2}$$

The barycenter X_2 is stationary at

$$\left[0, \frac{cb}{3a} \right]$$

Corollary 11. Over iso- X_2 triangles, the Nagel point X_8 is stationary at E 's center.

Proof. Direct from the location of the stationary barycenter and the fact that $|X_1X_8| = 3|X_1X_2|$ [37, Incenter, eqn.(11)]. In fact, $|X_1X_8| = 3(cb/(2a) - cb/(3a)) = cb/(2a) = |C_2|$. \square

Corollary 12. *The Spieker center X_{10} , incenter of the medial triangle and the midpoint of X_1 and X_8 [18] will be stationary on E 's minor axis.*

Observation 10. *Since X_2 is stationary, the family conserves $|X_1X_2|$, which for any triangle with sidelengths l_i is given by [37, Triangle Centroid, eqn.(11)]:*

$$|X_1 - X_2|^2 = -\frac{\sum l_i^3 + 9\prod l_i - 2(l_2l_1^2 + l_3l_1^2 + l_2^2l_1 + l_3^2l_1 + l_2l_3^2 + l_2^2l_3)}{9\sum l_i}$$

Lemma 3. *The barycenter X_2 of the MacBeath is stationary.*

Proof. The foci of the caustic are X_3 and X_4 , therefore X_2 must be fixed, $|X_3X_2| = |X_3X_4|/3$ [37, Triangle Centroid, eqn. (13)]. Consider also that MacBeath family are the intouch triangles of bicentric polygons (Chapple's porism). The X_2 of the intouch triangle is the Weill point X_{354} of the reference [18], shown to be stationary over the bicentric family [21, Thm. 4.1]. \square

Proposition 26. *Given an outer ellipse E centered on O and a point C in its interior, there is an (elliptic) caustic K centered on C such that over Poncelet, X_2 on OC is stationary.*

Referring to Figure 26:

Proof. Let \mathcal{A} be an affine transform that sends E to a circle E' . Let K' be the unique MacBeath caustic in E' with a first focus at its center and the other the reflection of E' about $C' = \mathcal{A}C$. Recall that conic centers are equivariant with respect to affinities. Let K be the image of K' under \mathcal{A}^{-1} . The X_2 of the family in (E, K) will be stationary because (i) the MacBeath's centroid is stationary, Lemma 3 and (ii) the centroid is the only triangle center which is equivariant with respect to affinities [18]. X_2 must lie on OC because affinities preserve collinearities. Notice it will nevertheless not lie on the major axis of K (foci are not equivariant). \square

7.3. **Focal-X(4).** Referring to Figure 25 (bottom left):

Proposition 27. *The orthocenter X_4 is stationary at a focus $f = [\pm c, 0]$ of E for the circular caustic with center and radius given by:*

$$C_4 = \left[\pm \frac{a^2c}{2a^2 - c^2}, 0 \right], \quad r_4 = \frac{a(a^2 - c^2)}{2a^2 - c^2}$$

Numeric search over the first forty-thousand triangle centers on [18] reveals:

Referring to Figure 27:

Observation 11. *For the focal- X_4 family the center (resp. other focus) of E is X_{7952} (resp. X_{18283}) on [18]. The locus of the circumcenter X_3 is an ellipse with a focus at E 's center. The locus of X_{20} is twice as large, with a focus on E 's distal focus.*

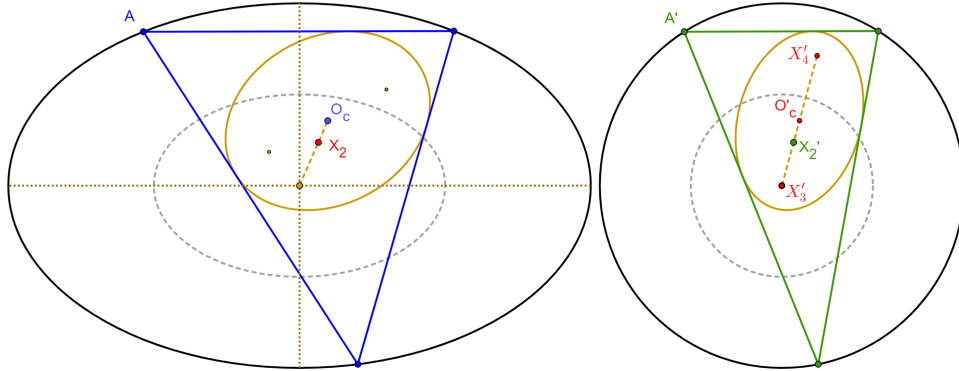


FIGURE 26. **left:** To find a caustic at a given center O_c that keeps X_2 stationary, find an affinity that sends the outer ellipse E' to a circle E' ; **right:** in such an affine projection find the MacBeath caustic with a focus at the center and another at the reflection of the latter about the projection of O_c under the affinity. The desired caustic on the left system is the image of said MacBeath caustic under the inverse affinity. Because affinities preserve collinearities, the stationary X_2 will lie on OO_c . [Video](#)

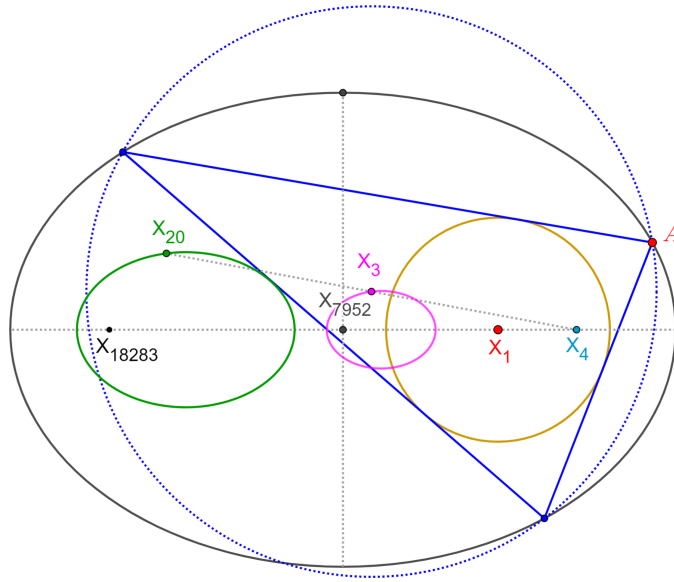


FIGURE 27. The focal- X_4 family: the outer ellipse E has foci on X_4 and X_{18283} and center on X_{7952} . Also shown are the loci of the orthocenter X_3 , with a focus on said center, and that of the de Longchamps point X_{20} (a reflection of X_4 on X_3), so twice as big, and with a focus on the other focus of E . [Video](#)

Definition 1. A triangle's *polar circle* is centered on X_4 and has squared radius given by [37, Polar Circle]:

$$r_{pol}^2 = 4R^2 - \frac{\sum l_i^2}{2}$$

This quantity is positive (resp. negative) for obtuse (resp. acute triangles).

Proposition 28. The focal- X_4 family conserves the (negative) squared radius of its polar circle at $r_{pol}^2 = -b^4/(a^2 + b^2)$.

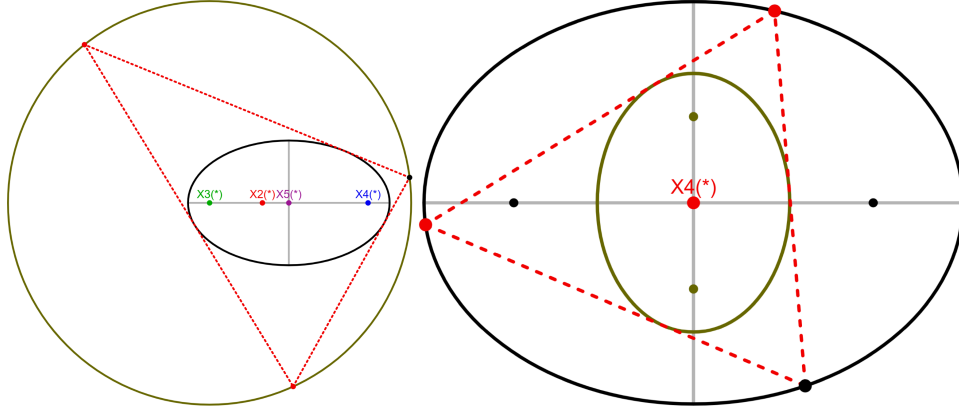


FIGURE 28. **left:** the ‘MacBeath’ family, **live;** **right:** the ‘dual’ family, **live.**

Proof. The incenter-orthocenter squared distance is given by [37, Incenter, eqn.(6)]:

$$(3) \quad |X_1 - X_4|^2 = 2r^2 + 4R^2 - \frac{\sum l_i^2}{2} = 2r^2 + r_{pol}^2$$

Since for this family $|X_1 X_4|$ is fixed as is the inradius r . The actual expression was obtained by CAS-based simplification. \square

Referring to Figure 28 (left):

Definition 2. The MacBeath Poncelet family is inscribed in a circle and circumscribes the MacBeath inconic, with foci at the circumcenter and its isogonal conjugate, the orthocenter. Its center is the Euler center X_5 , the midpoint of X_3 and X_4 [37, MacBeath inconic].

For the purposes of this section, let a, b denote the semiaxis’ lengths of the MacBeath inconic.

Lemma 4. *Over the MacBeath family, the sum of squared sidelengths, the sum of double-angle cosines, and the product of cosines are conserved. There are given by:*

$$\begin{aligned} \sum l_i^2 &= 9R^2 - |X_3 - X_4|^2 = 32a^2 + 4b^2 \\ \sum \cos(2\theta_i) &= \frac{c^2 - 3a^2}{2a^2} \\ \prod \cos \theta_i &= \frac{\sum l_i^2}{8R^2} - 1 = \frac{b^2}{8a^2} \end{aligned}$$

Proof. The first relation is direct from [37, Circumcenter, eqn.(6)], noting that the (i) the circumradius R is fixed and (ii) the caustic foci X_3, X_4 are stationary. The second one is obtained via CAS-simplification. The third one is direct from [37, Circumradius, eqn.(5)]. \square

Referring to Figure 28 (right):

Definition 3. The *dual* Poncelet family is interscribed between two dual ellipses [36]. They are also homothetic if one is rotated by 90-degrees.

Proposition 29. *The (i) MacBeath and (ii) dual families conserve $r_{pol}^2 < 0$. These are given by:*

$$r_{pol,macbeath}^2 = \frac{|X_3 - X_4|^2 - R^2}{2} = -2b^2$$

$$r_{pol,dual}^2 = -\frac{a^2b^2}{a^2 + b^2}$$

Proof. The first is direct from $|X_3 - X_4|^2 = 9R^2 - \sum l_i^2 = 2r_{pol}^2 + R^2$ [37, Orthocenter, eqn.(14)], noting that the MacBeath circumradius R is fixed and the caustic foci X_3 and X_4 are stationary. For the dual family, X_4 is stationary at the common center. Given the first relation it would therefore be sufficient to prove that $|X_3(t)|^2 - R^2(t)$ is constant. The final expression is obtained via CAS simplification. \square

Observation 12. *For the dual family the locus of the circumcenter X_3 is an ellipse homothetic to E with factor $c^2/(2(a^2 + b^2))$.*

Conjecture 4. *A Poncelet triangle family maintains X_4 stationary only if the conics are configured as focal- X_4 , MacBeath or Dual.*

7.4. **Iso- $X(7)$.** Referring to Figure 25 (bottom right):

Proposition 30. *For the circular caustic with center and radius given by:*

$$C_7 = \left[\frac{k_7}{2a}, 0 \right], \quad r_7 = \frac{b^2}{2a}$$

The Gergonne point will be stationary at:

$$X_7 = \left[\frac{2ak_7}{4a^2 - b^2}, 0 \right]$$

where $k_7 = \sqrt{4a^4 - 5a^2b^2 + b^4}$.

Observation 13. *The iso- X_7 family is the polar image of the Brocard porism [25, 31] with respect to the circumcircle, i.e., its tangential triangle. The former's stationary Gergonne point X_7 coincides with the stationary symmedian point X_6 of the Brocard porism [9].*

Proposition 31. *The family conserves the sum of half-angle tangents, given by:*

$$\sum_{i=1}^3 \tan \frac{\theta_i}{2} = \frac{\sqrt{4a^2 - b^2}}{a}$$

The $N > 3$ generalization of the Brocard porism is known as the Harmonic family, studied [12].

Conjecture 5. *The sum of half-angle tangents is also conserved for the polar image of the Harmonic family, for all $N > 3$.*

Since X_7 is stationary, the quantity $|X_1X_7|$ will also be conserved. For a generic triangle with semiperimeter s , this is given by [23, Corollary 4.2]:

$$|X_1 - X_7|^2 = r^2 \left(1 - \frac{3s^2}{(r + 4R)^2} \right)$$

Proposition 32. *Over Iso- X_7 triangles, this reduces to:*

$$|X_1 - X_7|^2 = \frac{b^4c^2}{4a^2(4a^2 - b^2)}$$

Definition 4. The Adams circle of a triangle is centered on X_1 and has radius R_A given by [37, Adams Circle]:

$$R_A = \frac{r\sqrt{\rho^2 - l_1l_2l_3s - \rho s^2}}{\rho - s^2}$$

where $\rho = l_1l_2 + l_2l_3 + l_3l_1$ and s is the semi-perimeter.

Proposition 33. The Iso- X_7 family conserves R_A and its value is given by:

$$R_A = \frac{b^2}{2a} \sqrt{\frac{5a^2 - b^2}{4a^2 - b^2}}$$

ACKNOWLEDGEMENTS

We would like to thank Arseniy Akopyan, Clark Kimberling, Peter Moses, and Richard Schwartz, for commenting on our developing results, encouraging us constantly, and providing insights and formulas. The second author is fellow of CNPq and coordinator of Project PRONEX/ CNPq/ FAPEG 2017 10 26 7000 508.

APPENDIX A. AFFINE TRIPLES

Triples α, β, γ used to express a given triangle center X_k as the linear combination $\alpha X_1 + \beta X_2 + \gamma X_3$, where $\rho = r/R$, reproduced from [17, Table 1]:

	X_1	X_2	X_3	X_4	X_5	X_7	X_8	X_9	X_{10}	X_{11}	X_{12}	X_{20}	X_{21}	X_{35}	X_{36}	X_{40}	X_{46}
α	1	0	0	0	0	$\frac{2\rho+4}{\rho+4}$	-2	$\frac{-\rho-2}{\rho+4}$	$-\frac{1}{2}$	$\frac{1}{1-2\rho}$	$\frac{1}{1+2\rho}$	0	0	$\frac{1}{2\rho+1}$	$\frac{1}{1-2\rho}$	-1	$\frac{1+\rho}{1-\rho}$
β	0	1	0	3	$\frac{3}{2}$	$\frac{3\rho}{\rho+4}$	3	$\frac{6}{\rho+4}$	$\frac{3}{2}$	$\frac{-3\rho}{1-2\rho}$	$\frac{3\rho}{1+2\rho}$	-3	$\frac{3}{2\rho+3}$	0	0	0	0
γ	0	0	1	-2	$-\frac{1}{2}$	$\frac{-4\rho}{\rho+4}$	0	$\frac{2\rho}{\rho+4}$	0	$\frac{\rho}{1-2\rho}$	$\frac{-\rho}{1+2\rho}$	4	$\frac{2\rho}{2\rho+3}$	$\frac{2\rho}{2\rho+1}$	$\frac{-2\rho}{1-2\rho}$	2	$\frac{-2\rho}{1-\rho}$

	X_{55}	X_{56}	X_{57}	X_{63}	X_{65}	X_{72}	X_{78}	X_{79}	X_{80}	X_{84}	X_{90}	X_{100}	X_{104}	X_{119}
α	$\frac{1}{1+\rho}$	$\frac{1}{1-\rho}$	$\frac{2+\rho}{2-\rho}$	$\frac{-\rho-2}{\rho+1}$	$\rho+1$	$-\rho-2$	$\frac{\rho+2}{\rho-1}$	1	$\frac{2\rho+1}{1-2\rho}$	$\frac{-\rho-2}{\rho}$	$\frac{-(\rho+1)^2}{\rho^2+2\rho-1}$	$\frac{2}{2\rho-1}$	$\frac{-2}{2\rho-1}$	$\frac{1}{2\rho-1}$
β	0	0	0	$\frac{3}{\rho+1}$	0	3	$\frac{-3}{\rho-1}$	$\frac{6\rho}{2\rho+3}$	$\frac{-6\rho}{1-2\rho}$	$\frac{6}{\rho}$	$\frac{6\rho}{\rho^2+2\rho-1}$	$\frac{-3}{2\rho-1}$	$\frac{3}{2\rho-1}$	$\frac{3\rho-3}{2\rho-1}$
γ	$\frac{\rho}{1+\rho}$	$\frac{-\rho}{1-\rho}$	$\frac{-2\rho}{2-\rho}$	$\frac{2\rho}{\rho+1}$	$-\rho$	ρ	0	$\frac{-6\rho}{2\rho+3}$	$\frac{2\rho}{1-2\rho}$	$\frac{2\rho-4}{\rho}$	$\frac{2\rho(\rho-1)}{\rho^2+2\rho-1}$	$\frac{2\rho}{2\rho-1}$	$\frac{2\rho-2}{2\rho-1}$	$\frac{-\rho+1}{2\rho-1}$

	X_{140}	X_{142}	X_{144}	X_{145}	X_{149}	X_{153}	X_{165}	X_{191}	X_{200}
α	0	$\frac{\rho+2}{2\rho+8}$	$\frac{-4\rho-8}{\rho+4}$	$\frac{4}{7}$	$\frac{-4}{6\rho-3}$	$\frac{4}{6\rho-3}$	$-\frac{1}{3}$	-1	$\frac{\rho+4}{\rho-2}$
β	$\frac{3}{4}$	$\frac{3\rho+6}{2\rho+8}$	$\frac{12-3\rho}{\rho+4}$	$\frac{3}{7}$	$\frac{-6\rho+9}{6\rho-3}$	$\frac{-6\rho-3}{6\rho-3}$	0	$\frac{6}{2\rho+3}$	$\frac{-6}{\rho-2}$
γ	$\frac{1}{4}$	$\frac{-2\rho}{2\rho+8}$	$\frac{8\rho}{\rho+4}$	0	$\frac{12\rho-8}{6\rho-3}$	$\frac{12\rho-4}{6\rho-3}$	$\frac{4}{3}$	$\frac{4\rho}{2\rho+3}$	0

APPENDIX B. LOCUS BEHAVIORS

Proposition 34. Over Poncelet triangles with a circular caustic, from X_1 to X_{1000} , X_k sweep a conic locus for the following k : 2, 3, 4, 5, 7, 8, 10, 11, 12, 20, 35, 36, 40, 42, 46, 55, 56, 57, 65, 79, 80, 81, 140, 145, 165, 171, 174, 176, 202, 213, 226, 354, 355, 365, 366, 367, 368, 370, 376, 381, 382, 388, 390, 396, 482, 484, 495, 496, 497, 498, 499, 506, 507, 546, 547, 548, 549, 550, 551, 553, 554, 559, 588, 590, 593, 597, 605, 609, 611, 612, 631, 632, 938, 939, 940, 941, 942, 944, 946, 950, 954, 955, 962, 975, 977, 980, 981, 989, 999, 1000.

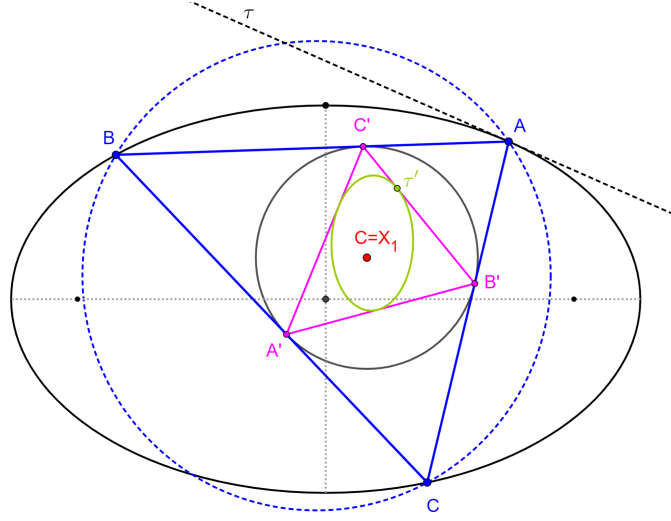


FIGURE 29. The contact family $A'B'C'$ is circle-inscribed and envelops a conic which is the polar image of tangents τ to \mathcal{E} with respect to the incircle. The point τ' indicated the instantaneous polarity.

Note that boldfaced entries above are triangle centers which are fixed combinations of X_2 and X_3 and will, over any Poncelet pair, sweep a conic locus [17].

Amongst some of the above-listed centers, six types of “locus behaviors” are observed:

- (1) **\mathcal{E} -homothety:** X_k , $k = 2$ (see [30]), 4, 8 (concentric), 10, 145, 368, 370, 551, 944, 946 are homothetic to \mathcal{E} .
- (2) **Axis alignment:** X_k , $k = 7, 79, 390, 1000$ are axis-aligned with E but not homothetic to it.
- (3) **C-focus:** X_k , $k = 5, 12, 355, 495, 496$ have C for a focus.
- (4) **C-major:** the major axis of X_k , $k = 3$ (foci on E 's axes), 35, 40, 55, 165 pass through C .
- (5) **C-minor:** the minor axis of X_k $k = 46, 56, 57, 999$ pass through C .
- (6) **Circle:** X_k , $k = 11$ (on incircle), 36, 65, 80 (centered on C), 354, 484, 942 are circles.

Pictures of the above can be found in [24].

APPENDIX C. FIXED CIRCUMCIRCLE FAMILY WITH EQUILATERAL

Referring to Figure 29, the family of contact triangles of a fixed incircle family is also Ponceletian: it is inscribed in a fixed circle and envelops the polar image of tangents to \mathcal{E} with respect to the incircle, also a conic [1]. In particular, it is easy to see that the original family contains an equilateral triangle if and only if the family of contact triangles contains an equilateral. Thus we shall now study Poncelet families of unit circle-inscribed triangles and the many phenomena that arise when they contain an equilateral triangle.

Let \mathcal{E}_c be an inconic with foci $f, g \in \mathbb{C}$, such that there is a Poncelet family of triangles inscribed in the unit circle \mathbb{T} and circumscribing \mathcal{E}_c . Referring to Figure 30:

Lemma 5. *A Poncelet family of triangles inscribed in the unit circle and circumscribing an ellipse with foci $f, g \in \mathbb{C}$ contains an equilateral triangle iff $1/f + 1/g$ is on the unit circle \mathbb{T} .*

Proof. First, assume that T_o is an equilateral triangle in this family. Let $\zeta \in \mathbb{T}$ be one of the vertices of T_o such that the other vertices are $e^{\frac{2\pi}{3}i}\zeta$ and $e^{\frac{4\pi}{3}i}\zeta$. Using the symmetric parameterization described in [Theorem 1](#), let $\lambda_o \in \mathbb{T}$ be the parameter corresponding to the triangle T_o . Plugging in the vertices in the parameterization, we get

$$\begin{aligned} f + g + \lambda_o \bar{f}\bar{g} &= \zeta + e^{\frac{2\pi}{3}i}\zeta + e^{\frac{4\pi}{3}i}\zeta = \zeta \left(1 + e^{\frac{2\pi}{3}i} + e^{\frac{4\pi}{3}i}\right) = 0 \\ \implies \lambda_o &= -\frac{(f+g)}{\bar{f}\bar{g}} \implies \left|-\frac{(f+g)}{\bar{f}\bar{g}}\right| = |\lambda_o| = 1 \\ \implies |f+g| &= |fg| \implies \left|\frac{1}{f} + \frac{1}{g}\right| = \left|\frac{f+g}{fg}\right| = 1 \end{aligned}$$

so $1/f + 1/g$ is on the unit circle \mathbb{T} , as desired.

Conversely, suppose that $1/f + 1/g$ is on the unit circle, that is, $|1/f + 1/g| = 1$. Rearranging, we have $|f+g| = |fg|$. Define $\lambda_o := -(f+g)/(\bar{f}\bar{g})$. Then

$$|\lambda_o| = \left|-\frac{(f+g)}{\bar{f}\bar{g}}\right| = \frac{|f+g|}{|\bar{f}\bar{g}|} = \frac{|f+g|}{|fg|} = 1$$

By definition, $f + g + \lambda_o \bar{f}\bar{g} = 0$. Moreover,

$$\begin{aligned} fg + \lambda_o(\bar{f} + \bar{g}) &= \lambda_o \bar{\lambda}_o fg + \lambda_o(\bar{f} + \bar{g}) = \lambda_o(\bar{\lambda}_o fg + \bar{f} + \bar{g}) = \\ &= \overline{\lambda_o(f + g + \lambda_o \bar{f}\bar{g})} = \lambda_o \bar{0} = 0 \end{aligned}$$

Hence, letting z_1, z_2, z_3 take the values of the 3 roots of $\zeta^3 = \lambda_o$, we see that these 3 roots form an equilateral triangle that satisfies the equations of the symmetric parameterization of [Theorem 1](#). Thus, this equilateral triangle is part of the Poncelet family, as desired. \square

Henceforth, let \mathcal{T}_o^* denote a Poncelet family of triangles interscribed between the unit circle and some inconic \mathcal{E}_c satisfying [Lemma 5](#).

Definition 5. The *Kiepert parabola* of a triangle is tangent to the three sides of a triangle. Its focus is X_{110} , always on the circumcircle, and its directrix is the Euler line X_2X_3 [\[37\]](#).

Still referring to [Figure 30](#), it follows from [Lemma 5](#):

Corollary 13. *Over \mathcal{T}_o^* , X_{110} is stationary at $(1/f + 1/g)^{-1}$.*

On [\[18\]](#), (i) the midpoint of X_3 and X_{110} is called X_{1511} , and (ii) X_{3233} is the vertex of the Kiepert inparabola [\[20\]](#). Referring to [Figure 31](#):

Observation 14. *Over \mathcal{T}_o^* , X_{3233} sweeps a circle with diameter $X_{110}X_{1511}$, i.e., $1/2$.*

Referring to [Figure 32](#), let A_{eq} be one of the vertices of the equilateral in \mathcal{T}_o^* . Let K be a chosen point on the circumcircle. Let \mathcal{B} represent the external bisector of $\angle KX_3A_{eq}$.

It can be shown:

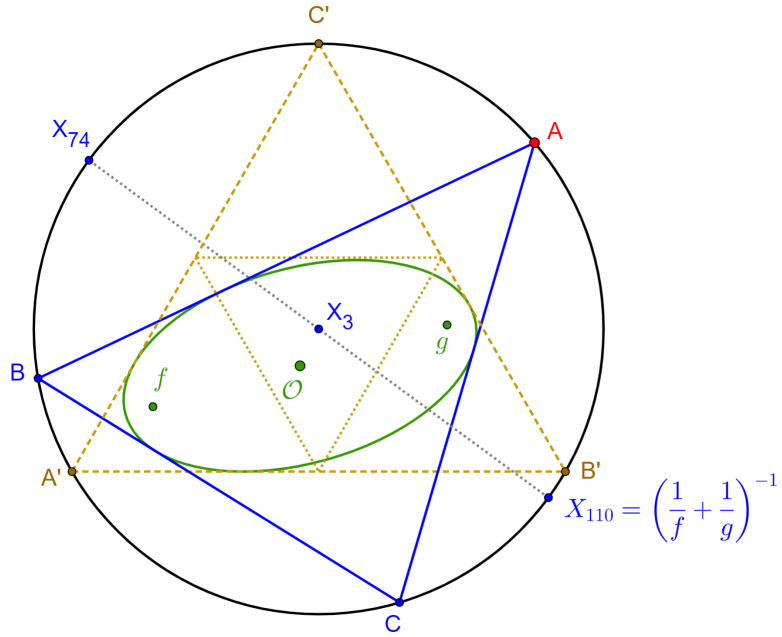


FIGURE 30. $T'_o = A'B'C'$ (brown) is an equilateral for which an inconic (green), centered at \mathcal{O} , is chosen, with foci at (complex) f, g . ABC is a triangle (blue) in the Poncelet family defined by the circumcircle (black) and the chosen inconic. Over the family, X_{110} , the focus of the Kiepert parabola (not shown) is stationary at $(1/f + 1/g)^{-1}$, as is its antipode X_{74} . [Video](#)

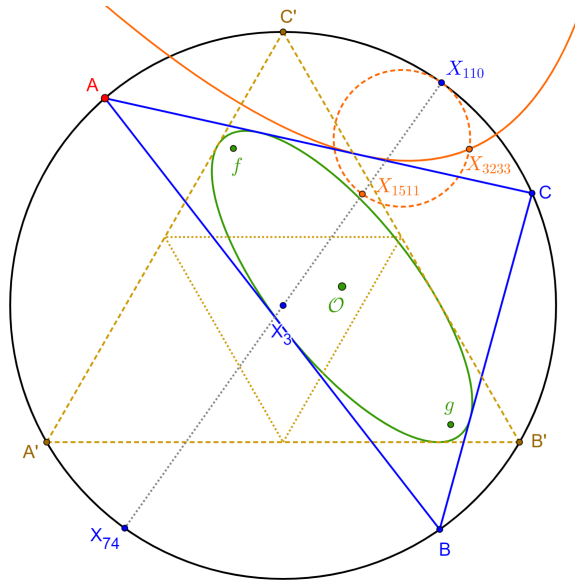


FIGURE 31. A $T_o = ABC$ in \mathcal{T}_o (blue) is shown (blue) along with its Kiepert parabola (orange), also an inconic, with focus at X_{110} . Over \mathcal{T}_o , the locus of its vertex X_{3233} is a circle (dashed orange) whose diameter is $X_{110}X_{1511}$. [Video](#)

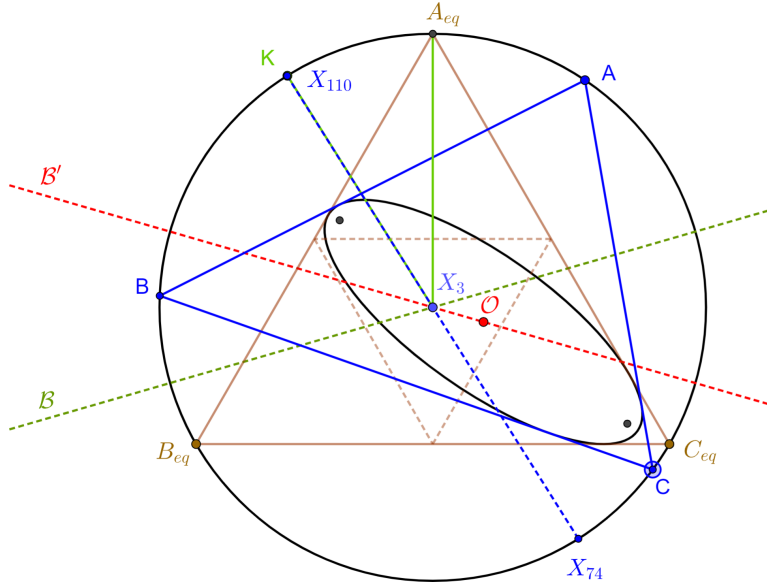


FIGURE 32. The construction in Proposition 35: K is chosen on the circumcircle; A_{eq} is a vertex of the equilateral; $T_o = ABC$ is a Poncelet triangle in \mathcal{T}_o^* ; \mathcal{B} (dashed green) is the external bisector of $\angle KX_3A_{eq}$; \mathcal{B}' (dashed red) is its reflection about X_3A_{eq} ; over all caustic centers \mathcal{O} on \mathcal{B}' , X_{110} is stationary, over \mathcal{T}_o^* , at the chosen K .

Proposition 35. *Over \mathcal{T}_o^* , X_{110} will be stationary at K for any \mathcal{O} on the reflection of \mathcal{B} about X_3A_{eq} .*

Referring to Figure 33, let $T_o = ABC$ be some generic triangle. Let \mathcal{O} be the center of an inconic \mathcal{E}_c . Let \mathcal{T}_o be the Poncelet family defined by the circumcircle and \mathcal{E}_c . Let \mathcal{L}_{35} be the perpendicular bisector of X_3X_5 .

It can be shown:

Proposition 36. *\mathcal{T}_o will contain an equilateral iff \mathcal{O} lies on \mathcal{L}_{35} . Furthermore, the stationary X_{110} is independent of \mathcal{O} .*

Let $\alpha = \angle X_{110}X_3\mathcal{O}$. Let \mathcal{O}' be the counterclockwise rotation of \mathcal{O} about X_3 by $\alpha/3 + \pi$. Still referring to Figure 33.

It can be shown:

Proposition 37. *One vertex of the equilateral contained in \mathcal{T}_o is located at the intersection of $X_3\mathcal{O}'$ with the circumcircle.*

Let \mathcal{T}'_o be the family of tangential triangles to \mathcal{T}_o , i.e., whose sides are tangent to the circumcircle at the vertices of T_o [37, Tangential Triangle]. Clearly, this family circumscribes a circle and will be inscribed in an ellipse \mathcal{E} , called above \mathcal{T} .

Observation 15. *\mathcal{E} is the polar image of the chosen inconic with respect to the circumcircle.*

Corollary 14. *Since the tangential of an equilateral is an equilateral, \mathcal{T}'_o will contain an equilateral, and therefore the center of its incircle will be on \mathcal{E}_{eq} .*

In turn, this leads to a restatement of Proposition 15:

$$\begin{aligned}
 & (a*b^2*(16*a^17*(b^4+22*b^2*yc^2+9*yc^4)+16*a*b^12*xc^2*(b^2-yc \\
 & \quad ^2)*(28*b^4-30*xc^2*yc^2+28*yc^4-b^2*(51*xc^2+56*yc^2))+8*a \\
 & \quad ^15*(35*b^6-36*xc^2*yc^4-2*b^4*(4*xc^2+175*yc^2)-3*b^2*(44* \\
 & \quad xc^2*yc^2+119*yc^4))+a^13*(-2559*b^8+144*xc^4*yc^4+b \\
 & \quad ^6*(-812*xc^2+2517*yc^2)+3*b^4*(32*xc^4+2168*xc^2*yc \\
 & \quad ^2+4945*yc^4)+3*b^2*(352*xc^4*yc^2+812*xc^2*yc^4+189*yc^6)) \\
 & +a^3*b^10*(64*b^8+60*xc^6*yc^2-1212*xc^4*yc^4+832*xc^2*yc \\
 & \quad ^6+64*yc^8-64*b^6*(73*xc^2+4*yc^2)+12*b^4*(573*xc^4+848*xc \\
 & \quad ^2*yc^2+32*yc^4)-b^2*(141*xc^6+6960*xc^4*yc^2+6336*xc^2*yc \\
 & \quad ^4+256*yc^6))+a^11*b^2*(2698*b^8+b^6*(5397*xc^2+18490*yc^2) \\
 & +18*b^4*(42*xc^4-983*xc^2*yc^2-1409*yc^4)-4*xc^2*yc^2*(88* \\
 & \quad xc^4-105*xc^2*yc^2+81*yc^4)-b^2*(64*xc^6+4608*xc^4*yc \\
 & \quad ^2+15699*xc^2*yc^4+2226*yc^6))+a^5*b^8*(112*b^8+8*b \\
 & \quad ^6*(1545*xc^2-22*yc^2)-3*b^4*(4991*xc^4+11960*xc^2*yc^2+48* \\
 & \quad yc^4)+b^2*(138*xc^6+22881*xc^4*yc^2+23064*xc^2*yc^4+368*yc \\
 & \quad ^6)+4*(3*xc^8+18*xc^6*yc^2-75*xc^4*yc^4+114*xc^2*yc^6-40*yc \\
 & \quad ^8))-a^7*b^6*(3876*b^8+b^6*(383*xc^2-6744*yc^2)-6*b \\
 & \quad ^4*(1897*xc^4+6571*xc^2*yc^2-288*yc^4)+3*b^2*(-85*xc \\
 & \quad ^6+9530*xc^4*yc^2+14813*xc^2*yc^4+424*yc^6)+4*(7*xc^8+171* \\
 & \quad xc^6*yc^2-756*xc^4*yc^4+483*xc^2*yc^6-33*yc^8))+a^9*b \\
 & \quad ^4*(9097*b^8-b^6*(14218*xc^2+26815*yc^2)+b^4*(-3105*xc \\
 & \quad ^4+300*xc^2*yc^2+14943*yc^4)+b^2*(-196*xc^6+15861*xc^4*yc \\
 & \quad ^2+39894*xc^2*yc^4+2811*yc^6)+4*(4*xc^8+226*xc^6*yc^2-639* \\
 & \quad xc^4*yc^4+354*xc^2*yc^6-9*yc^8))-192*b^11*xc^2*(b^2-yc^2) \\
 & ^2*d-128*a^14*b*(b^2+3*yc^2)*d+192*a^12*b*(2*b^4+4*xc^2*yc \\
 & \quad ^2+3*yc^4+b^2*(2*xc^2+23*yc^2))*d-4*a^2*b^9*(80*b^6-75*xc \\
 & \quad ^4*yc^2+144*xc^2*yc^4-80*yc^6-120*b^4*(7*xc^2+2*yc^2)+3*b \\
 & \quad ^2*(79*xc^4+232*xc^2*yc^2+80*yc^4))*d+12*a^10*b*(258*b \\
 & \quad ^6-32*xc^4*yc^2+33*xc^2*yc^4-b^4*(79*xc^2+1116*yc^2))-2*b \\
 & \quad ^2*(16*xc^4+193*xc^2*yc^2+211*yc^4))*d+12*a^4*b^7*(168*b \\
 & \quad ^6+5*xc^6-99*xc^4*yc^2+178*xc^2*yc^4-48*yc^6-2*b^4*(577*xc \\
 & \quad ^2+192*yc^2)+b^2*(263*xc^4+1320*xc^2*yc^2+264*yc^4))*d-12*a \\
 & \quad ^6*b^5*(47*b^6+15*xc^6-90*xc^4*yc^2+102*xc^2*yc^4-25*yc^6-b \\
 & \quad ^4*(1130*xc^2+799*yc^2)+b^2*(232*xc^4+2404*xc^2*yc^2+777*yc \\
 & \quad ^4))*d-4*a^8*b^3*(2579*b^6-32*xc^6-54*xc^4*yc^2+129*xc^2*yc \\
 & \quad ^4+9*yc^6+3*b^4*(31*xc^2-447*yc^2)-3*b^2*(62*xc^4+1570*xc \\
 & \quad ^2*yc^2+949*yc^4))*d)/((a^2-b^2)^2*(16*a^6-9*b^4*xc^2-8*a \\
 & \quad ^4*(b^2+2*xc^2)+a^2*b^2*(b^2+24*xc^2-yc^2))*(-(a^2*b^2*(8*b \\
 & \quad ^2+xc^2-24*yc^2))+a^4*(b^2-9*yc^2)+16*(b^6-b^4*yc^2))^2)
 \end{aligned}$$

where: $d = \sqrt{(a^4 - a^2*xc^2 + b^2*xc^2)*(b^4 + a^2*yc^2 - b^2*yc^2)}$. The expression for the minor semi-axis b_7 is the above where (a, b) and (x_c, y_c) are permuted.

APPENDIX E. TABLE OF SYMBOLS

symbol	meaning
$\mathcal{E}, \mathcal{E}_c$	Poncelet conics (incidence and tangency)
a, b, c	semi-axis' and half-focal lengths of \mathcal{E}
a_c, b_c, c_c	idem for \mathcal{E}_c
$\mathcal{K}, C = (x_c, y_c)$	incircle and its center (= X_1)
T, l_i, θ_i	a Poncelet triangle, sidelengths, and internal angles
r, R	inradius and circumradius of a T
$\mathcal{E}_{eq}, a_{eq}, b_{eq}$	(elliptic) locus of \mathcal{E} -inscr. equilat. centroids and semi-axes
X_k	triangle center indexed in Kimberling's [18]
X_1	Incenter: meet of angle bisectors
X_2	Barycenter: meet of medians
X_3	Circumcenter: meet of perpendicular bisectors
X_4	Orthocenter: meet of altitudes
X_5	Center of Euler's (9-pt) circle
X_7	Gergonne point: perspector of the contact triangle
X_8	Nagel's point: perspector of the extouch triangle
X_{11}	Feuerbach's point: touchpoint of incircle and Euler's circle
X_{36}	circumcircle-inverse of X_1
X_{59}	isogonal conjugate of X_{11}
X_{80}	reflection of X_1 on X_{11}
$C_i = (x_i, y_i), a_i, b_i$	center and semiaxes of the (elliptic) locus of X_i 's
F_i, F'_i	foci of the (elliptic) locus of X_i
X_i^*	stationary X_i
\mathcal{T}	Poncelet triangle family about the incircle
\mathcal{L}_k	locus of X_k over \mathcal{T}
\mathcal{T}^*	the family \mathcal{T} containing an equilateral
\mathcal{T}_g	Poncelet triangle interscribed between two generic conics
\mathcal{T}_o	circle-inscribed Poncelet triangle family
\mathcal{T}_o^*	the family \mathcal{T}_o containing an equilateral
\mathcal{T}'_o	tangential triangles to \mathcal{T}_o^* , identical to \mathcal{T}^*
f, g	foci of caustic of \mathcal{T}_o
λ	parameter of symmetric parametrization [4]

TABLE 2. Symbols used in the article. For geometric constructions for the X_i , see [37].

REFERENCES

- [1] Akopyan, A. V., Zaslavsky, A. A. (2007). *Geometry of Conics*. Providence, RI: Amer. Math. Soc. 32
- [2] Bellio, F., Garcia, R., Reznik, D. (2022). Parabola-inscribed Poncelet polygons derived from the bicentric family. *J. Croatian Soc. for Geom. & Gr. (KoG)*, 26. 26

- [3] del Centina, A. (2016). Poncelet's porism: a long story of renewed discoveries i. *Arch. Hist. Exact Sci.*, 70(2): 1–122. doi.org/10.1007/s00407-015-0163-y. 1
- [4] Daepf, U., Gorkin, P., Shaffer, A., Voss, K. (2019). *Finding Ellipses: What Blaschke Products, Poncelet's Theorem, and the Numerical Range Know about Each Other*. MAA Press/AMS. 3, 5, 38
- [5] Darlan, I., Reznik, D. (2021). An app for visual exploration, discovery, and sharing of Poncelet 3-periodic phenomena. 4
- [6] Davis, P. J. (1995). The rise, fall, and possible transfiguration of triangle geometry: A mini-history. *Am. Math. Monthly*, 102(3): 204–214. 4
- [7] Dragović, V., Radnović, M. (2011). *Poncelet Porisms and Beyond: Integrable Billiards, Hyperelliptic Jacobians and Pencils of Quadrics*. Frontiers in Mathematics. Basel: Springer. books.google.com.br/books?id=QcOmDAEACAAJ. 1, 4
- [8] Fierobe, C. (2021). On the circumcenters of triangular orbits in elliptic billiard. *J. Dyn. Control Syst.* [doi:10.1007/s10883-021-09537-2](https://doi.org/10.1007/s10883-021-09537-2). 1
- [9] Garcia, R., Reznik, D. (2021). Family ties: Relating Poncelet 3-periodics by their properties. *J. Croatian Soc. for Geom. & Gr. (KoG)*, 25(25): 3–18. <https://hrcak.srce.hr/en/clanak/390431>. 9, 30
- [10] Garcia, R., Reznik, D. (2024). The conic locus of the isogonal conjugate of a point with respect to generic Poncelet triangles. *TBD*. In preparation. 18, 19
- [11] Garcia, R., Reznik, D., Koiller, J. (2023). Loci of 3-periodics in an elliptic billiard: why so many ellipses? *J. Symb. Computation*, 114(4): 336–358. 1, 3, 17, 24
- [12] Garcia, R., Reznik, D., Roitman, P. (2022). New properties of harmonic polygons. *J. Geom. Graphics*, 26(2): 41–60. 30
- [13] Georgiev, V., Nedyalkova, V. (2012). Poncelet's porism and periodic triangles in ellipse. *Dynamat*. www.dynamat.orw.eu/upload_pdf/20121022_153833_0.pdf. 1
- [14] Glutsyuk, A. (2014). On odd-periodic orbits in complex planar billiards. *J. Dyn. Control Syst.*, 20(3): 293–306. doi.org/10.1007/s10883-014-9236-5. 1
- [15] Helman, M., Garcia, R., Reznik, D. (2024). Locus of the orthocenter over generic Poncelet triangles. *TBD*. In preparation. 8
- [16] Helman, M., Laurain, D., Garcia, R., Reznik, D. (2021). Invariant center power and loci of Poncelet triangles. *J. Dyn. & Contr. Sys.* 4, 5, 6, 24
- [17] Helman, M., Laurain, D., Reznik, D., Garcia, R. (2022). Poncelet triangles: a theory for locus ellipticity. *Beitr. Algebra Geom.* 1, 3, 4, 6, 7, 31, 32
- [18] Kimberling, C. (2019). Encyclopedia of triangle centers. faculty.evansville.edu/ck6/encyclopedia/ETC.html. 1, 3, 10, 15, 18, 21, 27, 33, 36, 38
- [19] Kimberling, C. (2020). Central lines of triangle centers. bit.ly/34vVoJ8. 15
- [20] Moses, P. (2024). Vertex of the Kiepert inparabola. Private Communication. 33
- [21] Odehnal, B. (2011). Poristic loci of triangle centers. *J. Geom. Graph.*, 15(1): 45–67. 1, 2, 24, 25, 27
- [22] Ogilvy, C. S. (1969). *Excursions in Geometry*. New York: Oxford Univ. Press. 21
- [23] Queiroz, J. F. (2021). Gergonne's point and outstanding distances. Romanian Mathematical Magazine. <https://www.ssmrmh.ro/wp-content/uploads/2021/07/GERGONNES-POINT-AND-OUTSTANDING-DISTANCES.pdf>. Florică Anastase (ed.). 30
- [24] Reznik, D. (2024). Six nifty behaviors of loci of Poncelet triangles with a circular caustic. ResearchGate. https://www.researchgate.net/publication/382637554_Six_nifty_behaviors_of_loci_of_Poncelet_triangles_with_a_circular_caustic. 32
- [25] Reznik, D., Garcia, R. (2022). A matryoshka of Brocard porisms. *European J. of Math*, 8: 308–329. 30
- [26] Reznik, D., Garcia, R., Koiller, J. (2020). The ballet of triangle centers on the elliptic billiard. *J. Geom. Graphics*, 24(1): 079–101. 1, 17
- [27] Reznik, D., Garcia, R., Koiller, J. (2020). Can the elliptic billiard still surprise us? *Math Intelligencer*, 42: 6–17. rdcu.be/b2cg1. 2
- [28] Roitman, P., Garcia, R., Reznik, D. (2021). New invariants of Poncelet-Jacobi bicentric polygons. *Arnold Math. J.*, 7(4): 619–637. 26
- [29] Romaskevich, O. (2014). On the incenters of triangular orbits on elliptic billiards. *Enseign. Math.*, 60(3–4): 247–255. arxiv.org/pdf/1304.7588.pdf. 1, 24
- [30] Schwartz, R., Tabachnikov, S. (2016). Centers of mass of Poncelet polygons, 200 years after. *Math. Intelligencer*, 38(2): 29–34. www.math.psu.edu/tabachni/prints/Poncelet5.pdf. 8, 32

- [31] Shail, R. (1996). Some properties of brocard points. *The Mathematical Gazette*, 80(489): 485–491. [30](#)
- [32] Sirfoga, U. (2014). Equilateral triangle inscribed in a ellipse. Mathematics Stack Exchange. math.stackexchange.com/q/769819. [12](#)
- [33] Skutin, A. (2013). On rotation of a isogonal point. *J. of Classical Geom.*, 2: 66–67. jgeometry.org/Articles/Volume2/JCG2013V2pp66-67.pdf. [18](#)
- [34] Stanev, M. (2019). Locus of the centroid of the equilateral triangle inscribed in an ellipse. *International Journal of Computer Discovered Mathematics (IJCDM)*, 4: 54–65. [3](#), [12](#)
- [35] Tabachnikov, S. (2005). *Geometry and Billiards*, vol. 30 of *Student Mathematical Library*. Providence, RI: American Mathematical Society. Mathematics Advanced Study Semesters, University Park, PA. [1](#)
- [36] Walker, R. J. (1978). *Algebraic Curves*. New York: Springer. [29](#)
- [37] Weisstein, E. (2019). Mathworld. *MathWorld—A Wolfram Web Resource*. mathworld.wolfram.com. [3](#), [7](#), [9](#), [18](#), [21](#), [22](#), [23](#), [27](#), [28](#), [29](#), [30](#), [31](#), [33](#), [35](#), [38](#)